Total Gaseous Mercury (TGM) measurements at the Cape Verde Atmospheric Observatory (CVAO)

Luis Silva Mendes Neves

MSc by Research

University of York

Chemistry

July 2014

Abstract

Atmospheric mercury has been claimed by UNEP to be the second most important global environmental issue after greenhouse gases, and many countries are becoming increasingly concerned about atmospheric mercury pollution.

Transported in the atmosphere in the form of gaseous elemental mercury (GEM), which is the less reactive form and accounts for more than 95% of total gaseous mercury (TGM), it has a 0.5 – 2 year residence time in the atmosphere. This lifetime makes it an important global pollutant, recorded as persistent and bio-accumulative toxic, after oxidation processes that culminates in deposition to the surface environment and aquatic food chain, causing several types of damage to human health and ecosystems.

Presented here the results from the first two years of total gaseous mercury measurements at the Cape Verde Atmospheric Observatory. These are made as part of the Global Mercury Observation System (GMOS) network, the goal of which is to establish long-term continuous world coverage of mercury measurements. This project contributes high precision data that is representative for a large geographical area in the tropical Atlantic Ocean. Up until now the only existing data in this region have been from short-term ship-based cruise campaigns. The observatory is located at 16.86403º N, 24.86752º W (10 m a.s.l.), approximately 50 m from the coastline, there are no habitation within a 2 km radius and the nearest public road is 1.2 km downwind. The prevailing wind is from the NE from the open ocean bringing air masses from the tropical Atlantic and from the African continent. Measurements made in 2012 and 2013 were broadly consistent with previously published measurements in the region, with typical atmospheric values of between 1.0 and 1.5 ng m^{-3}. Whilst located in the Northern hemisphere, the low latitude of Cape Verde resulted in observations more similar in concentration to those reported previously in the Southern hemisphere. Gaseous Hg showed little annual variability at Cape Verde, (slight minimum in November and December, and maximum from July to September), but had a strong diurnal cycle with a minimum in the later afternoon. The destruction of Hg during the day was consistent with loss mechanisms by bromine and hydroxyl (OH), which both have maxima during the day. Many synoptic scale events (1-5 days) showed a close relationship between observed mercury and other tracers of long-range pollution transport e.g. CO, or a strong dependence on air mass origin, seen for example during Saharan dust transport.

List of Contents

List of Tables

List of Figures

Preface

The report, now presented as a master thesis is not just the result of the last two and a half years of hard work with this project, but the culminating of a long journey that started eight years ago when I first step in the laboratories at the Cape Verde Atmospheric Observatory in Calhau, São Vicente. It was then, the start of an enriching, exciting and challenging experience that drove me to the middle of the world atmospheric scientific community, and from where I´ve been learning a lot, getting new skills and experience on running scientific equipment and taking part on many scientific researches activities, from daily routine laboratory work and field campaigns to international workshops and conferences. The demands and responsibilities of the position showed me the need to be more prepared for the challenge that is being involved and being part of this high standard research working group, and working on this master project was the opportunity to start looking with different eyes to the whole science produced at the CVAO, by looking not just at the performing aspects of the monitoring equipment and data quality but going much deeper on data analyses and scientific research, with the first results showed now at the present report.

Acknowledgements

I want to thank all the people involved with the CVAO activities during the last eight years that directly or indirectly took part and make possible for me to be involved with this project.

I would like to express special thanks the National Institute of Meteorology and Geophysics, (INMG) and its staff, Ester, Bruno, Gisela and Helder for all the support, the incentives and for their daily work.

I would like to thank the Max Planck Institute staff, Martin, Lena, Reimo and Thomas for all the support during those years of this joining work.

I would like to thank the Leibniz Institute for Tropospheric Research staff, Hartmut, Konrad, Thomas, Wadinga and Nicole for all the support during those years of this joining work.

I would like to acknowledge the University of York for this opportunity, with special thanks to Lucy for the incentives, special thanks to Ally and James that guided me while doing this report and for all the incentives, to Shalini for her supporting work, and a very special thanks to Katie for everything, I´ve learn a lot with you during all those years.

I have no words to express my gratitude to my parents, my Father and my Mother that long time ago left behind their house, their family, their friends and their home island with the unique objective of searching for better opportunities of education for me, my brothers and my sisters. I want to thank you for a whole life of unconditional support; I want to thank you for everything. Congratulations, you really did a great job, I love you all.

Author declaration

I declare that this thesis is a presentation of original work and I am the sole author. This work has not previously been presented for an award at this, or any other, University. All sources are acknowledged as references.

1. Introduction

Mercury, primarily because of its existence and bioaccumulation as methylmercury in aquatic organisms, is a concern for the health of higher trophic level organisms, or to their consumers. This is the major factor driving current research in mercury and global environmental regulation. This is the driver for the UNEP Global Partnership for Mercury Transport and Fate Research initiative, whose goal is to assess the relative importance of different processes or mechanisms affecting the transfer of mercury (Hg) from emission sources to aquatic and terrestrial receptors and provide possible source-receptor relationships. This transfer occurs through atmospheric transport, chemical transformations and subsequent deposition, and involves the intermittent recycling between reservoirs that occurs prior to ultimate removal of Hg from the atmosphere. Understanding sources, global Hg transport and fate, and the impact of human activity on the biosphere, requires improved knowledge of Hg movement and transformation in the atmosphere. An improved understanding of Hg emission sources, fate and transport is important if there is to be a focused and concerted effort to set priorities and goals for Hg emissions management and reduction at the national, regional and global levels, and to develop and implement such policies and strategies.

Mercury is ubiquitous in the atmosphere and the ground-level background concentrations appear to be relatively constant over hemispheric scales (Pirrone and Mason, 2008), varying by less than a factor of two for remote locations. This is expected for a trace gas that has a relatively long residence time in the atmosphere. The southern hemisphere has a lower concentration than the northern hemisphere and this primarily reflects the current and historic concentration of anthropogenic emissions in the northern hemisphere. Recent measurements of free tropospheric air, either at high altitude sites or from measurements made on board aircraft, indicate that the concentration changes are usually but not always also relatively small vertically up to the tropopause, although there are differences apparent between measurement campaigns. In the stratosphere, Hg has been found associated with the stratospheric aerosol. Mercury fate and transport in the boundary layer is complex, and its concentration is modified by inputs and removal to the terrestrial/ocean surface. In addition, rapid global transport of Hg can occur in the free troposphere. The fate of Hg is therefore determined by the different chemical environments that these regions of the atmosphere represent, the different physical and meteorological processes which occur in

them, the differences in chemical reactivity, and also by exchange that occurs between reservoirs (Pirrone et al. 2005; Hedgecock et al. 2006; Lindberg et al. 2007).

Anthropogenic inputs of Hg have greatly exacerbated the global Hg cycle. Much of this impact is related to energy resources exploitation, especially fossil fuel consumption. The impact of these enhanced emissions is such that atmospheric concentrations have increased by a factor of three on average since pre-industrial times. Globally, fossil fuel power plants are the single most important anthropogenic emission source of Hg to the atmosphere, and these emissions, in combination with the emission of other co-emitted pollutants, have an impact on the atmospheric chemistry of Hg and influence its resultant deposition patterns. While the primary impacts are observable in the short term, the medium to long term impact that exploitation of fossil fuels and other anthropogenic activities have on atmospheric Hg cycling is through their impact and influence by global climate change (Hedgecock and Pirrone, 2004; Eisenreich et al. 2005).

An understanding of the different mercury sources is also of importance towards assessing control options since many different mercury sources exist. In addition to anthropogenic point sources, natural sources also exist and mercury once released into the environment can be extensively recycled between different compartments of the environment. In Fig 1, a schematic description of the main source types is presented.

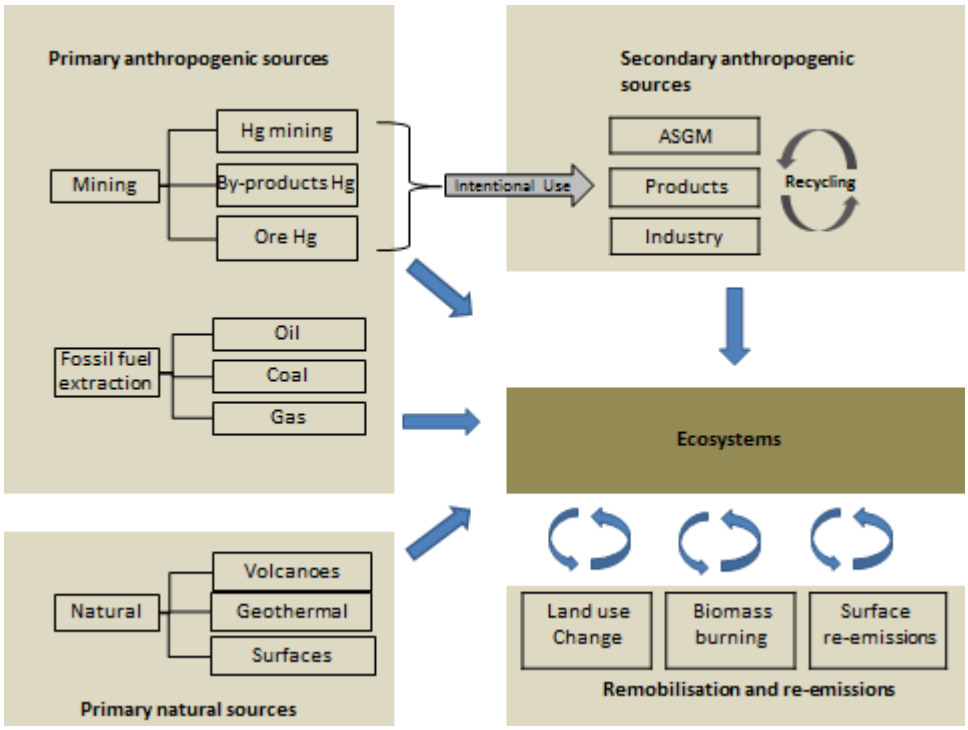

Figure 1. *Schematic description of emission source types and remobilization processes affecting mercury distribution in the environment. Blue arrows represent the release of mercury and subsequent transport and input to ecosystems.*

The *primary anthropogenic sources* are those where mercury of geological origin is mobilized and released to the environment. The two main source categories of this type are mining (either for mercury or where mercury is a by-product or contaminant in the mining of other minerals) and extraction of fossil fuels where mercury is present as a trace contaminant

The *secondary anthropogenic sources* are those where emissions occur from the intentional use of mercury, e.g., industry, products or for artisanal gold mining. In both these source types, emissions to the environment can occur via direct discharges of exhaust gases and effluents, although the generation of mercury-containing waste also contributes.

Primary natural sources, are defined as those where mercury of geological origin is released via natural processes such as volcanoes or geothermal processes or evasion from natural surfaces geologically enriched in mercury. In addition to these source types, the distribution of mercury is affected by its remobilization and re-emission pathways. In the latter case, mercury released can be of either natural or anthropogenic origin and it is currently not possible to experimentally distinguish between the two. Anthropogenic

activities such as biomass burning and land use changes will affect the magnitude and location of the mercury releases.

Oceans and seas are the largest natural emitters (Pirrone et al., 2009) of mercury to the atmosphere but in a general global budget for mercury in the environment proposed by Sunderland and Mason (2007), some 6000 t/yr of mercury are emitted to the atmosphere, whereas only 600 t/yr are transported via rivers to the sea. The atmosphere therefore represents the dominant fast pathway for the transport of mercury in the environment.

By mass, the largest emitted Hg species to the atmosphere is gaseous elemental mercury (GEM), with minor amounts emitted as oxidized mercury either as oxidized mercury in the gas phase (also termed reactive gaseous mercury; RGM) or as oxidized mercury associated with particles (total particulate mercury; TPM). GEM has a relatively long lifetime in the atmosphere (currently believed to be between 0.5 and 1.5 years), being slowly oxidized to either RGM or TPM, and thus, mercury is ubiquitous in the troposphere. RGM and TPM have much shorter lifetimes (hours to days) and are therefore subject to fast removal by wet or dry deposition. Consequently, the RGM and TPM emitted from primary sources tends to be regional in its effect (i.e., tends to be deposited closer to sources), although under certain conditions some TPM may be subject to long range transport.

The chemistry of mercury in the troposphere is complex and involves both gas phase reactions and aqueous phase reactions. In comprehensive reviews (Calvert and Lindberg, 2005; Lin et al., 2006; Ariya et al., 2008; Steffen et al., 2008) information from studies concerning the most important reactions of GEM have been compiled, and this is summarized in the table 1.

The atmospheric reactions of mercury are critical to determining how mercury is transported in the atmosphere and where it is deposited. As previously stated, the long lifetime of GEM makes it a global pollutant, whereas RGM and TPM are deposited locally or regionally. Because of the local removal of RGM and TPM, the highest depositions of mercury are found close to emission sources in Europe, North America and East Asia (Christensen et al., 2004; Dastoor and Larocque, 2004).

There is ongoing scientific debate about the reactions that may be responsible for removing GEM from the atmosphere and large efforts have been devoted to the study of the chemical removal of GEM.

Experimental evidence has shown that GEM can be oxidized by species such as ozone, hydroxyl or halogens radicals (Holmes et al., 2010; Pal and Ariya, 2004; Stephens et al., 2012). Ozone is produced photo-chemically from the reaction between hydrocarbons and nitrogen oxides, from both anthropogenic and natural sources. However, these studies only focus on the first step of the reaction sequences leading to RGM and so, may overestimate the conversion of GEM to RGM (Goodsite et al., 2004; Calvert and Linberg, 2005; Ariya et al., 2007).

GEM may also be transported to particles and oxidized by ozone in the particles (Munthe, 1992). The reaction with OH is leading to an HgOH intermediate. This intermediate was found to be short-lived and thermal decomposition could be its dominating fate, which indicates that the reaction with OH is of minor importance (Calvert and Lindberg, 2005; Goodsite et al., 2004). The direct reaction between O_3 and GEM to form HgO is endothermic and thus, is not occurring in the atmosphere (Calvert and Lindberg, 2005). However, Hg might still react with O_3 to form an HgO_3 intermediate that can react further, for example heterogeneously. This discussion is based on limited scientific data and more investigations are needed.

The gas phase reaction of GEM with bromine (Br) is emerging as an important reaction in the global atmosphere. This reaction starts a sequence of reactions that eventually lead to RGM. Measurements of reactive gaseous mercury (RGM; primarily gaseous Hg(II)) in the polar (Simpson et al., 2007; Steffen et al., 2008) to sub-tropical MBL (Laurier et al., 2003; Laurier and Mason, 2007; Obrist et al., 2011) and global mercury transport modelling (Holmes et al., 2010; Soerensen et al., 2010b) have suggested that the oxidation of Hg(0) in the MBL is primarily by atomic bromine (Br), which is produced photolytically from Br-containing compounds and through the Br/BrO cycle involving tropospheric O3 (Saiz-Lopez and von Glasow, 2012). The currently held bromine-induced elemental mercury oxidation scheme (reactions R6-R9, table 1) is thought to involve a Hg(I) intermediate HgBr (Goodsite et al., 2004, 2012; Holmes et al., 2010). This reaction sequence is temperature-dependent (Goodsite et al., 2004) and the fastest removal of GEM is observed under cold conditions such as those prevailing at the polar regions or in the upper part of the troposphere, where the HgBr intermediate formed is stable enough to undergo further oxidation to Hg(II) (Goodsite et al., 2004, 2012). The contribution of Bromine to Hg(I)-to-Hg(II) oxidation in the tropical MBL is, however, expected to be of lesser importance, since reactive bromine concentration are generally low in the tropical regions (Theys et

al., 2011) and since the HgBr intermediate tends to dissociate readily under warm temperatures (Goodsite et al., 2004, 2012; Dibble et al., 2012). In the background troposphere only small fluctuations in GEM concentrations are observed (Kim and Kim, 1996; Ebinghaus et al., 2002; Weiss-Penzias et al., 2003), which agrees well with a relatively long atmospheric lifetime of Hg obtained in a model study (Holmes et al., 2006).

Bromine atoms can be produced from a number of sources: one is sea spray and is thus connected to the marine boundary layer; a second source is refreezing leads (open water areas in sea ice or between sea ice and the shore) during polar spring, where Br_2 is released from bromide-enriched sea-ice surfaces. Thirdly, Br can be produced in the upper part of the troposphere from the photolysis of organo-bromides.

If the lifetime of GEM in the atmosphere were less than 0.5 years then there must be reduction reactions in the atmosphere to ensure a sufficiently long residence time of mercury to explain the uniform concentrations of GEM observed there. Photolytic reduction or reduction by reaction with HO_2 (hydroperoxyl or perhydroxyl) radicals are the two main pathways (Lin et al., 2006) suggested. However it has been shown that these reactions are too slow under atmospheric conditions to be important (Gardfeldt and Jonsson, 2003; Lin et al., 2006).

Several authors have discussed a number of possible oxidation and reduction reactions for RGM in aqueous aerosol, but it is likely that most important process is the conversion of different TPM species into mercuric chloride ($HgCl_2$) which may subsequently re-evaporate (Gardfeldt and Jonsson, 2003; Lin et al., 2006). Once GEM is oxidized to RGM and/or TPM, the mercury is subject to fast removal from the atmosphere by either dry or wet deposition.

In general, compounds that are persistent in the environment (i.e., are not readily chemically-degraded), that have a long atmospheric lifetime and a high vapor pressure can be transported globally, whereas those with medium vapor pressure tend to remain (deposit) within the source region, and compounds with low vapor pressure tend to deposit locally. In the group of components with medium vapor pressure, some compounds can be re-emitted and be transported over longer distances by the “multi-hop” (or grasshopper) effect.

Deposited mercury can be converted back to elemental mercury by chemical reactions (reduction reactions) in the soil or water or by bacteria, or alternatively can be converted by bacteria to methyl mercury, but in either case, the result may be re-emission of mercury to the atmosphere. Mercury is therefore one of the pollutants that can be transported by a so-called "multihop" process involving repeated cycles of transport–deposition–re-emission. One result of this is that mercury, even mercury originally emitted as RGM or TPM and deposited close to sources, can be transported towards colder regions (where re-emission is less pronounced).

Polar regions – In 1998, Schoroeder and co-workers published results from Alert, Canada showing GEM being depleted from the atmosphere close to the surface in episodes during polar springtime (Schoroeder et al., 1998). These episodes were therefore termed atmospheric mercury depletion events (AMDEs). AMDEs were observed to occur together with depletion of ozone, which had been observed for the first time some years earlier (et all., 1988). These observations led to a series of laboratory, field and theoretical studies of possible reactions of GEM, and today there is no doubt that the principal reaction in AMDEs is between GEM and Br. In the Arctic, the lifetime of GEM is about 10 hours because the reactions initiated by Br are faster at low temperatures. This lifetime corresponds to a Br concentration of 0.7 pptv at an average temperature of 245 K (Goodsite et al., 2004), which is well within the range of Br concentration of 0.2 to 6 pptv that were observed (Tuckermann et al., 1997). The bromine-initiated reaction lead to RGM (Lindberg et al., 2002; Brooks et al., 2006a) or TPM (steffen et al., 2003) formation, the RGM and/or TPM being then (rapidly) removed to the surface, from which it may be subsequently re-emitted.

The production of atmospheric Br is closely connected to refreezing leads where bromide is pushed out to the surface during the refreeze of seawater. AMDEs are only observed when the temperature is below -4 ^{o}C over sea ice and when solar light is present (Lindberg et al., 2002).

These reactions between mercury and Br occur in marine-influenced air, thus deposition of mercury is enhanced in Arctic coastal areas during polar springtime (Douglas et al., 2005). It has been estimated that AMDEs enhance the deposition of mercury in polar regions by about 120 t/yr, from 80 t/yr that would be expected from normal deposition, to about 200 t/yr.

A central issue in relation to the mercury cycle and also for potential impacts on biota is how much of the deposited mercury enters the food web, how much is removed to sediments, and how much is re-emitted to the atmosphere. This is still the subject of scientific debate and study with estimates of the amount of deposited mercury that is re-emitted currently ranging from ca. 20 to 95% (Aspmo et al., 2006; Brooks et al., 2006a; Steffen et al., 2008). High levels of mercury have been observed in snow at Barrow, Alert and Ny-Alesund following AMDEs but these decrease strongly after the AMDEs (Aspmo et al., 2006). AMDEs are nearly always followed by periods where the GEM signal is elevated, which is assumed to reflect re-emission. Different opinions regarding the extent to which deposited mercury is re-emitted may reflect geographical differences within the Arctic.

Mid- and equatorial latitudes – GEM oxidation results at the production of divalent species Hg(II) that are very soluble and can be deposited by precipitation or incorporated to particulate matter (TPM). However, the mechanism of Hg(0) oxidation in the marine boundary layer (MBL) and its subsequent removal are not well known, particularly in the tropical oceans (Strode et al., 2007; Sorensen et al., 2010a).

Mercury dynamics in the tropical MBL is of interest as the upwelling of colder and nutrient-rich waters in these regions is known to be associated with enhanced mercury evasion from the oceans, presumably due to phytoplanckton´s conversion of seawater Hg(II) to Hg(0) (Fitzgerald et al., 1984; Kim and Fitzgerald, 1986), but can also be due to photochemical reduction of seawater Hg(II) (Sorensen et al., 2010b, 2013). Continuous monitoring of total gaseous mercury at a tropical Atlantic coastal site in Surinam did not detect any mercury evasion signal (Muller at al., 2012). Global mercury modelling has also resulted in highly contradictory estimates: an earlier model suggested that oceanic mercury emissions are largest in the tropics (Strode et al., 2007), but the net oceanic mercury emission from the tropical ocean was much less in a more recent estimate (Sorensen et al., 2010b).

An indication that bromine atoms may not be the only important oxidant for mercury in the tropical MBL can be observed in a recent round-the-globe cruise study (Soerensen et al., 2010a). Although generally low, the peak RGM concentration at a few sites in the MBL of the tropical Atlantic and Pacific oceans were similar to those observed in the sub-tropical and temperate regions (Soerensen et al., 2010a). As the concentrations of atomic chlorine

in the MBL are very low (≤ 104 atoms cm-3) Platt et al., 2004), one plausible candidate oxidant would be atomic iodine (I), which is predicted to aid in rapid oxidation of the HgBr intermediate (reaction R10 in Table 1) (Goodsite et al., 2004, 2012). Indeed, a role of iodine-containing species in RGM formation has been implied by modelling studies in the polar regions (Saiz-Lopez et al., 2008; Calvert and Lindberg, 2004), but has not been experimentally confirmed or quantified. Quantum chemical calculations have recently suggested that the HgBr intermediate could also be further oxidized in the presence of other free radicals such as NO2, HO2, ClO, and BrO (reactions R12-R16 in Table 1) (Dibble et al., 2012).

In the Marine boundary layer, bromine is produced from sea spray. At a temperature above 290 K and Br concentrations of 0.1 ppt typical for the marine boundary layer at mid-latitudes this corresponds to an atmospheric lifetime for GEM of more than 4000 hours (ca. 0.45 years) and thus Br has the potential to be the most important oxidant for the removal of GEM from the atmosphere.

The photochemical degradation of organo-bromides increases with height, and organo-bromides are the dominant Br source above an altitude corresponding to 300 hpa. The source strength and mechanisms are discussed by Yang et al. (2005) together with the geographical distribution of bromine sources and bromine compounds. The parameterization of atmospheric bromine compounds is thus very important for a reliable description of the dynamics of atmospheric mercury. Yang and co-workers found the uncertainty to be a factor of 2 for the description of the formation of sea salt particles alone.

Based on this information, it can be concluded that the gas phase reactions of GEM with Br most probably control the atmospheric lifetime of atmospheric mercury outside the Polar Regions. In the background troposphere, only small fluctuations in GEM concentrations are observed (Kim and Kim, 1996; Ebinghaus et al., 2002; Weiss-Penzias et al., 2003), which agrees well with the relatively long atmospheric lifetime of mercury obtained by Holmes et al. (2006). However, it has to be noted that there are still large uncertainties in the description of the GEM oxidation process and there is a strong need for experimental studies of the reactions between GEM and atmospheric Oxidants.

The annual average concentration of GEM observed in the European and North American troposphere at background sites(i.e., unaffected by local sources) is between 1.5 and 1.7

ng/m^3, slightly higher than but similar to the 1.2 to 1.4 ng/m^3 found at sites in the southern hemisphere(e.g., the monitoring site in South Africa). In East Asia, the regional value for GEM is higher, with a mean of close to 4 ng/m^3 (Kim, 2004) thought to reflect proximity to the major emission sources in the Asian region. Close to sources, higher levels of GEM are measured and concentrations of up to 5μg/m^3 (5000 ng/m^3) have been measured at Almaden, Spain close to an old silver mine (Ferrara et al., 1998).

By comparison, RGM concentration in Europe and North America (south of the Artic) are found levels of up to around 40 pg/m^3, and TPM at levels up to around 60 pg/m^3 (Walberg et al., 2001).

The highest levels of RGM have been measured at Point Barrow, Alaska, at around 1000 pg/m^3 (Brooks et al., 2006a). In another Artic study, at Alert, Canada, the maximum levels of RGM measured were around 40 pg/m^3, and TPM around 100 pg/m^3 (Cobbet et al., 2007).

Table 1. *Gas-phase mercury-halogen reactions used in photochemical box models*

Reaction	Rate constant (1 atm) cm^3 molecule $^{-1}$ s^{-1}	Reference
Direct oxidation scheme		
(R1) $Hg^0 + O_3 \rightarrow Hg^{II}O + O_2$	3×10^{-20}	Hall (1995)
(R2) $Hg^0 + OH \rightarrow Hg^{II}$	$3.55 \times 10^{-14} e^{-2440/RT}$	Pal and Ariya (2004)
(R3) $Hg^0 + Br_2 \rightarrow Hg^{II}Br_2$ [a]	9.0×10^{-17}	Ariya et al. (2002)
(R4) $Hg^0 + BrO \rightarrow Hg^{II}O + Br$	1×10^{-15}	Raofie and Ariya (2003)
(R5) $Hg^0 + ClO \rightarrow Hg^{II}O + Cl$	1×10^{-17}	Subir et al. (2011)
Two-step oxidation scheme		
(R6) $Hg^0 + Br \rightarrow Hg^{I}Br$	$1.1 \times 10^{-12} (T/298)^{-2.37}$	Goodsite et al. (2004)
(R7) $Hg^{I}Br \rightarrow Hg^0 + Br$	$1.2 \times 10^{10} e^{-8357/T}$	Goodsite et al. (2004)
(R8) $Hg^{I}Br + OH \rightarrow Hg^{II}BrOH$	$2.5 \times 10^{-10} \times (T/298)^{-0.57}$	Goodsite et al. (2004)
(R9) $Hg^{I}Br + Br \rightarrow Hg^{II}Br_2$	$2.5 \times 10^{-10} \times (T/298)^{-0.57}$	Goodsite et al. (2004)
(R10) $Hg^{I}Br + I \rightarrow BrHg^{II}I$	$2.5 \times 10^{-10} \times (T/298)^{-0.57}$	Goodsite et al. (2004)
(R11) $Hg^0 + Cl (+Y) \rightarrow Hg^{I}Cl + Y$	$2.2 \times 10^{-32} e^{680(1/T - 1/298)}$	Donohoue et al. (2005)
Updated two- steps oxidation scheme		
(R6´) $Hg^0 + Br \rightarrow Hg^{I}Br$	$3.7 \times 10^{-13} (T/298)^{-2.76}$	Goodsite et al. (2012)
(R7´) $Hg^{I}Br \rightarrow Hg^0 + Br$	$1.6 \times 10^{-9} e^{-7801/T} \times [M]$	Dibble et al. (2012)
(R8´) $Hg^{I}Br + OH \rightarrow BrHg^{II}OH$	6.33×10^{-11}	
(R9´) $Hg^{I}Br + Br \rightarrow Hg^{II}Br_2$	6.33×10^{-11}	
(R10´) $Hg^{I}Br + I \rightarrow BrHg^{II}I$	6.28×10^{-11}	
(R11) $Hg^0 + Cl (+Y) \rightarrow Hg^{I}Cl + Y$	$2.2 \times 10^{-32} e^{680(1/T - 1/298)}$	
(R12) $Hg^{I}Br + NO_2 \rightarrow BrHg^{II}NO_2$	2.81×10^{-11}	
(R13) $Hg^{I}Br + NO_2 \rightarrow BrHg^{II}ONO$	5.82×10^{-11}	
(R14) $Hg^{I}Br + OH_2 \rightarrow BrHg^{II}HO_2$	8.2×10^{-11}	
(R15) $Hg^{I}Br + BrO \rightarrow BrHg^{II}OBr$	1.09×10^{-11}	
(R16) $Hg^{I}Br + IO \rightarrow BrHg^{II}OI$	4.9×10^{-11}	
Henry´s law constant (equilibrium)		
(R17) $HgCl_2 = HgCl_2(aq)$	1.4×10^6 M atm^{-1}	Hedgecock and Pirrone (2001)

1.1. The Environmental impacts of mercury

While some pollutants are restricted in their range and in the size and number of population they affect, mercury is not one of them. Wherever it is mined, used or discarded, it is liable, in the absence of effective disposal methods, to finish up thousands of kilometers away because of its propensity to travel through air and water. Beyond that, it reaches the environment more often after being unintentionally emitted than through negligence in its disposal. The prime example of this is the role played by the burning of fossil fuels and biomass in adding to mercury emissions.

Once released, mercury can travel long distances, and persists in environments where it circulates between air, water, sediments, soil, and living organisms. Mercury is concentrated as it rises up the food chain, reaching its highest level in predator fish such as swordfish and shark that may be consumed by humans. There can also be serious impacts on ecosystems, including reproductive effects on birds and predatory mammals. High exposure to mercury is a serious risk to human health and to the environment.

Air emissions of mercury are highly mobile globally, while aquatic releases of mercury are more localized. Mercury in water becomes more biologically dangerous and eventually some mercury evaporates into the atmosphere. Once deposited in soils and sediments, the mercury changes its chemical form, largely through metabolism by bacteria and other microbes, and becomes methylmercury, the most dangerous form for human health and the environment. Methylmercury normally accounts for at least 90 per cent of mercury in fish. Methylmercury is a problem for several reasons. First, it is taken up by plankton much more efficiently than is inorganic mercury, resulting in concentrations in plankton that are as high as 10,000 times the concentration in seawater. Second, methylmercury is absorbed through the intestines of animals much more easily than inorganic mercury. Third, methylmercury biomagnifies as it moves up the food web. Thus, methylmercury becomes an increasingly greater proportion of the mercury in organisms higher in the food web.

Mercury can enter the food chain either from agricultural products or from seafood. It was widely used in agriculture, and at least 459 people are known to have died in Iraq after grain treated with a fungicide containing mercury was imported in 1971 and used to make flour (Greenwood, 1985). Those who showed the greatest effect were the children of women who had eaten contaminated bread during pregnancy. Though many of these acute cases are now in the past, agricultural products may still contain mercury. The institute for

agriculture and trade policy in USA recently found that high fructose corn syrup (used in sodas, ketchup and bread) could also contain elevated mercury levels (Default et al., 2009). Another study suggested that in an area marked by intensive mercury mining and smelting and heavy coal-powered industry, rice crops could be contaminated (Zhang et al., 2010).

Human groups at risk include the millions of ASGM (artisanal and small-scale gold mining) miners across the world, where mercury compounds are used in production. However, a far greater number of people whose main source of protein is fish or other marine creatures may be exposed to contamination (UNEP-WHO, 2008). The Food and Agriculture Organisation says: "Just over 100 million tonnes of fish are eaten world-wide each year, providing two and a half billion people with at least 20 per cent of their average per capita animal protein intake. This contribution is even more important in developing countries, especially small islands states and in coastal regions, where frequently over 50 per cent of people´s animal protein comes from fish. In some of the most food- insecure places – many parts of Asia and Africa, for instance – fish protein is absolutely essential, accounting for a large share of an already low level of animal protein consumption" (FAO, 2010).

The once pristine Arctic region is a special environmental case. About 200 tonnes of mercury are deposited in the Arctic annually, generally far from where it originated. A 2011 report by the Arctic Monitoring and Assessment Program (AMAP) reported that mercury levels are continuing to rise in some Arctic species, despite reductions over the past 30 years in emissions from human activities in some parts of the world. It reports a ten-fold increase in the last 150 years in levels in belugas, ringed seals, polar bears and birds of prey. Over 90 per cent of the mercury in these animals, and possibly in some Arctic human populations, is therefore believed to have originated from human sources. The average rate of increase wildlife over the past 150 years is one to four per cent annually: " The fact that trends are increasing in some marine species in Canada and West Greenland despite reductions in North American emissions is a particular cause for concern, as these include species used for food" (AMAP, 2011). A recent study of preschool children in three regions of the Arctic showed that almost 59% of children exceeded the provisional tolerable weekly intake (PTWI) level for children (Tian et al., 2011; WHO, 1998).

Mercury can seriously harm human health, and is a particular threat to the development of fetuses and young children. If affects humans in several ways. As vapour it is rapidly absorbed into the blood stream when inhaled. It damages the central nervous system, thyroid, kidneys, lungs, immune system, eyes, gums and skin. Neurological and behavioural disorders may be signs of mercury contamination, with symptoms including tremors, insomnia, memory loss, neuromuscular effects, headaches, and cognitive and motor dysfunction. Recent studies have also shown mercury to have cardiovascular effects (McKelvery and Oken, 2012). In the young it can cause neurological damage resulting in symptoms such as mental retardation, seizures, vision and hearing loss, delayed development, language disorders and memory loss. The Inuit population of Quebec has among the highest levels of exposure to mercury of any population in the world. It has been recently concluded that children with higher levels of contamination are more likely to be diagnosed with attention deficit hyperactivity disorder (Boucher et al., 2012).

In cases of severe mercury poisoning, as occurred in the Minamata case in Japan, symptoms can include numbness in the hands and feed, general muscle weakness, narrowing of the field vision, and damage to hearing and speech. In extreme cases, insanity, paralysis, coma and death have been known to ensue rapidly. People may be at risk of inhaling mercury vapour from their work (in industry of ASGM), or in spills, and may be at risk through direct contact of mercury with the skin. The most common form of direct exposure for humans, however, is through consuming fish and sea food contaminated with methylmercury. Once ingested, 95 per cent of the chemical is absorbed in the body. Source (Mercury, Time to act – UNEP)

1.2. Uses of Mercury

Mercury has been used since antiquity. Archaeologists have recovered traces from Mayan tombs and from the remains of Islamic Spain (Bank, 2012). The first emperor of unified China is said to have died after ingesting mercury pills intended to give him eternal life (Asia History website). Metallic mercury is still used in some herbal and religious remedies in Latin America, Asia and Caribbean rituals (ATSDR, 1999).

Even now, mercury still used extensively in daily life. Electrical and electronic devices, switches (including thermostats) and relays, measuring and control equipment, energy

efficient fluorescent light bulbs, batteries, mascara, skin lightening creams and other cosmetics which contain mercury, dental fillings and a host of other consumables are used across the globe. Food products obtained from fish, terrestrial mammals and other products such as rice can contain mercury. It is still widely used in health care equipment, where much of it is used for measuring, and in blood pressure devices and thermometers, although their use is declining. There are safe and cost-effective replacements for mercury for many health care applications and for pharmaceuticals, and goals have been set to phase out some mercury-containing devices altogether. For instance, the UNEP Mercury Products Partnership, a mechanism for delivery of immediate actions, has set the goal of reducing demand for mercury-containing fever thermometers and blood pressure devices by at least 70 per cent by 2017.

In 2005, UNEP estimated global annual mercury demand at between 3,000 and 3,900 tonnes (UNEP, 2006). Demand has fallen significantly in the last 50 years, from 9,000 tonnes a year in the 1960s to 7,000 in the 1980s and 4,000 a decade later(UNEP, 2006). A growing understanding of the risks posed by the toxicity of mercury, the increasing availability of substitutes and international action mean that many uses of mercury are now disappearing. Source (Mercury, Time to act – UNEP)

1.3. The Global Mercury Observation System (GMOS)

The Global Mercury Observation System (GMOS) is a 5 year project, funded by the European Commission 7th Framework Programme, which is establishing a worldwide observation system for measurement of atmospheric mercury in ambient air and precipitation samples. GMOS include ground-based monitoring stations (Fig.2), shipboard measurements over the Pacific and Atlantic Oceans, European Seas, as well as aircraft based measurements from the ground to the lower atmosphere.

GMOS data will be used to test regional and global scale atmospheric mercury models, which can then be used for determining the current state of atmospheric mercury contamination, and its deposition to ecosystems. This will enable the development of policies to minimize ecosystem risk from mercury pollution.

The first mercury measurements were made just 30 years ago, and since then measurements have generally been sporadic and confined to just a few geographical

locations. To provide recommendations which help minimize the risk to human and ecosystem health from mercury, it is necessary to know how the concentration and deposition flux of mercury changes over time, and with location.

GMOS has been conceived in order to establish the infrastructure, methodologies and data repository to begin the task of characterizing the spatio-temporal variations in atmospheric mercury species concentrations and deposition fluxes.

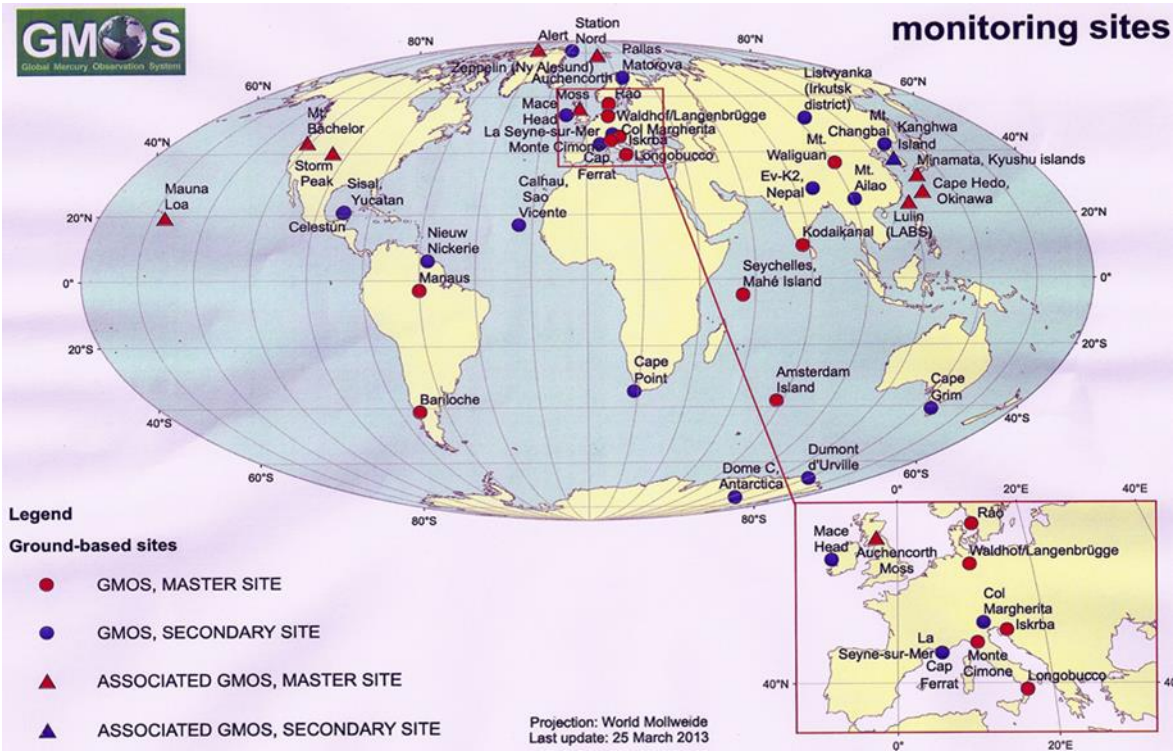

Figure 2. GMOS *land-based monitoring stations. Calhau station, São Vicente (CVAO) seen in the center of global map.*

Current mercury observation networks are limited and consistent techniques are not adopted on global scales in the same way that they are for greenhouse gases and priority pollutants such as ozone. In addition, as for any atmospheric contaminant, it is not feasible to perform enough measurements to determine with precision global concentration patterns.

The overall goal of the GMOS is to develop a coordinated global observation system for mercury, including ground-based stations at high altitude and sea level locations, ad-hoc oceanographic cruises over the Pacific, the Atlantic and the Mediterranean, and free tropospheric mercury measurements. This will then provide high quality data for the

validation and application of regional and global scale atmospheric models, to give a firm basis for future policy development and implementation.

The specific objectives of the GMOS are:

- To establish a Global Observation System for Mercury able to provide ambient concentrations and deposition fluxes of mercury species around the world, by combining observations from permanent ground-based stations, and from oceanographic and tropospheric measurement campaigns.
- To validate regional and global scale atmospheric mercury modelling systems able to predict the temporal variations and spatial distributions of ambient concentrations of atmospheric mercury, and Hg fluxes to and from terrestrial and aquatic receptors.
- To evaluate and identify source-receptor relationships at country scale and their temporal trends for current and projected scenarios of mercury emissions from anthropogenic and natural sources.
- To develop interoperable tools to allow the sharing of observational and model output data produced by GMOS, for the purposes of research and policy development and implementation as well as at enabling societal benefits of Earth Observations, including advances in scientific understanding in the nine Societal Benefit Areas (SBA) established in GEOSS.

As one of the partners of the GMOS monitoring network, the Cape Verde Atmospheric Observatory, CVAO (Calhau station) is contributing with high precision data that could be representative for this large geographical area in the tropical Atlantic Ocean where until the start of GMOS monitoring activities the only existing data available were from short-term ship-based cruise campaigns.

2. Experimental

2.1. The Cape Verde Atmospheric Observatory (CVAO)

Measurements are made at the Cape Verde Atmospheric Observatory (Calhau station) one of the major WMO Global Atmosphere Watch stations (Fig.3) that measure a wide range of atmospheric parameters such as O_3, CO, NO, NO_2, NOy, and VOCs. Measurements started with the start of operations at the site in October 2006. Chemical characterisation of aerosol measurements and flask sampling of greenhouse gases began in November 2006, halocarbon measurements in May 2007, and physical measurements of aerosol in June 2008. On-line measurements of greenhouse gases (CH_4, CO_2, N_2O, CO, SF_6) began in October 2008. In 2011 CVAO became part of the Global Mercury Observation System(GMOS) network, and from December 2011 on, Total gaseous Mercury (TGM) measurements has started, and recently, during July 2014 a wet precipitation collector for mercury analyzes were installed at the site.

Figure 3. *Map of the WMO GAW atmospheric network, Cape Verde observatory, seen in the centre of the global map.*

Figure 4. *Cape Verde Atmospheric Observatory located at Calhau, São Vicente Island in Cape Verde*

The station is located at São Vicente island (Fig 4) in Cape Verde, 16.86403º N, 24.86752º W (10 m a.s.l.), approximately 50 m from the coast line. There are no habitations within a 2 km radius and the nearest public road is 1.2 km downwind. The prevailing wind is from the NE from the open ocean bringing air masses from the tropical Atlantic, from the west coast of Africa, Europe and North America.

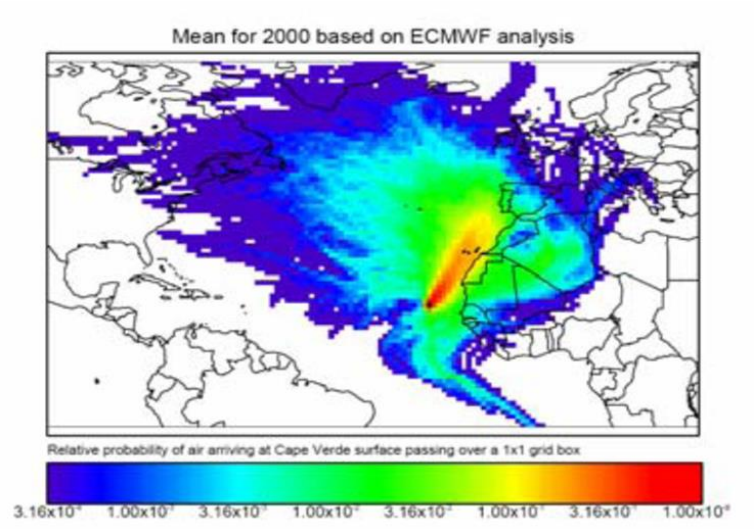

Figure 5. *Wind trajectory probability distribution for 2000 showing the overwhelming effect of the NE trade winds.*

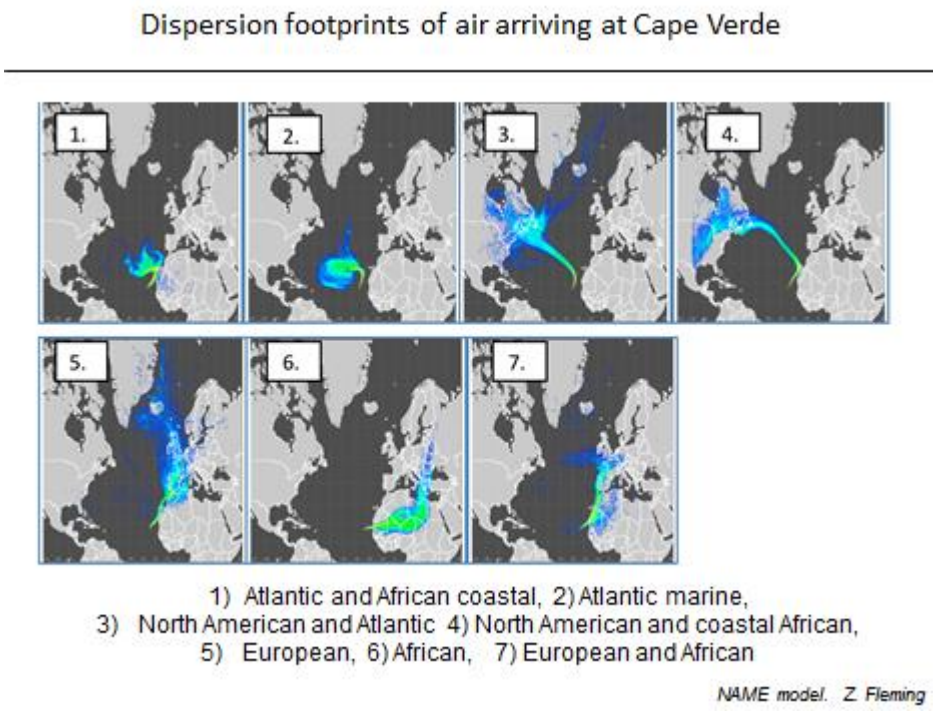

Figure 6. *Geographic origins (past 5 days) of air masses arriving at the Cape Verde Atmospheric Observatory*

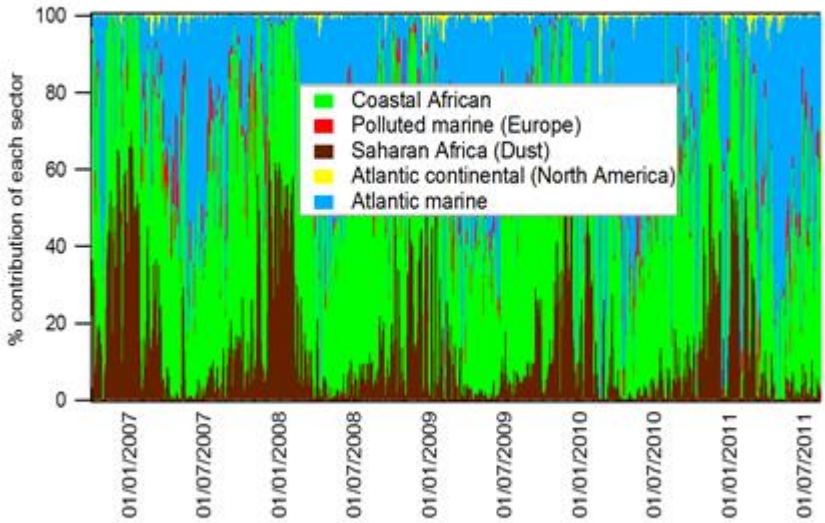

Figure 7. *Contribution of main footprints to the air arriving at CVAO*

Figure 8. *Cape Verde Atmospheric Observatory, A Global Atmospheric Watch station*

Figure 9. *Analyzers for continuous measuring of Ozone (O_3), Carbon monoxide (CO) and total gaseous mercury (TGM) at the Cape Verde Atmospheric Observatory - CVAO*

Fig 10. *Wet precipitation collector for analysis of mercury content in precipitation samples installed in July 2014*

2.2. Total Gaseous Mercury measurements

Key details of instrumentation and measurements are given in the table (table2), below, and a longer description follows:

Table 2. *Key details of instrumentation and measurements*

Continuous Ambient Hg Measurements
Instrumentation: TEKRAN 2537 B Hg Vapor Analyzer (dual gold cartridge sampling/desorption and CVAFS detection)
Measurement: Continuous analysis of Total Gaseous Mercury (TGM) in air at ng/m³ levels.
Sample frequency: 5 min

Air is sampled from a glass inlet placed at 10 m high outside of the Lab (Fig 11), and then drawn into the containerized lab using a sample pump. In the lab, the inlet is heated and a Teflon line with a particulate filter takes the sample to the instrument.

Figure 11. *Photo shows the glass inlet line from 10 meter sampling tower and pathway into the laboratory.*

Figure 12. *TEKRAN mercury analyzer, Model 2537B*

The instrument (Fig. 12) samples air and traps mercury vapor into a cartridge containing an ultra-pure gold adsorbent. The amalgamated mercury is then thermally desorbed and detected using Cold Vapour Atomic Fluorescence Spectrometry (CVAFS). A dual cartridge design allows alternate sampling and desorption, resulting in continuous measurement of the air stream. Mercury is released from the traps when they are heated by the trap heating coils. It is important that the A and B traps demonstrate internally consistent measurements. Oscillating concentrations values between traps indicates a problem with one of the traps or their heating coils. The sample time for each cartridge is set to 300 sec according to GMOS Standard Operating Procedures (SOPs).

A 2537 pump is set to a constant flow rate that is monitored in real-time to ensure that the pump is functioning correctly and the correct amount of ambient air is being sampled. A precision mass flow meter (MFC) is used to meter sample flow rate through the cartridge. A microcomputer integrates flow rates over time to provide the total volume of air measured for each sample. Sample flow is typically set to 1 L min^{-1}, with a total of 5L for each sample. During the first year of measurements it was set to 1,5 L min^{-1} with a total sample volume of 7,5 L.

To check the performance of the flow meter, calibrations are performed against external measures such as bubble meters. Below shows a calibration on the 26th September 2013. Different flows were set at the instrument flow meter, with the same flow being measured 20 times by the calibrator, giving at the end a flow average for each. Results are displayed at Fig 11 plot, showing a linear variation of the flow as expected.

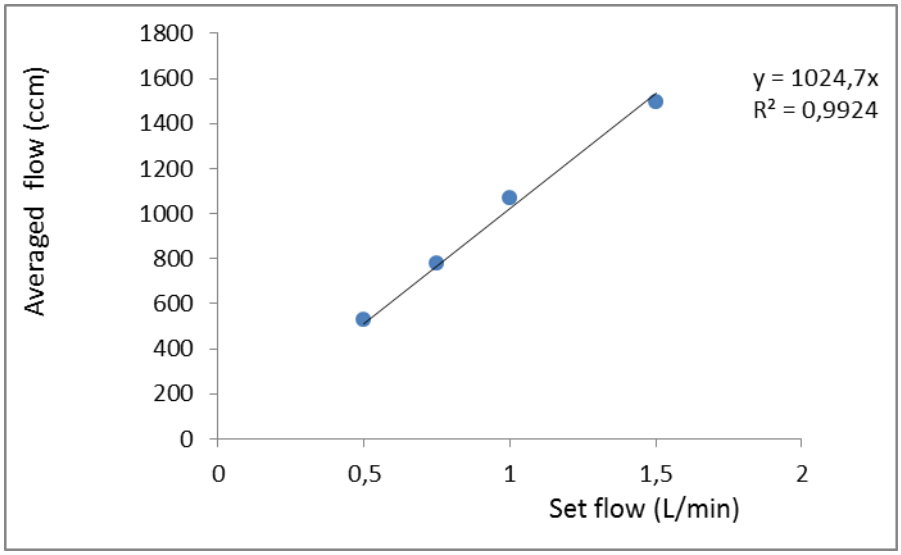

Figure 13. *Flow meter calibration plot for TGM analyzer at Cape Verde*

The instrument has provision for two methods of chemical calibrations. The first is a manual injection of gas from a mercury vapour permeation source. The second method is via an automatic internal permeation source calibration. In the Cape Verde instrument this is set to calibrate automatically every 71 hours. The internal calibration consists of a zero and span (where a known amount of mercury is released from the permeation source) for each trap. Each calibration result is examined to confirm that the system is performing at an appropriate level of data TGM data quality. Since the internal automatic calibration has functioned well over two years, there has been no requirement to use manual injection this far.

Argon, grade 4.8 is used as a carrier gas with the delivery pressure set to 50psi. Mercury is swept from the gold traps directly to the analyzer using Argon gas (note there is no chromatographic separation in this process). The 2537 TEKRAN analyzer ceases sampling and goes into Idle mode if the Argon pressure decreases to less than 200 psi.

The analyzer section of the instrument is equipped with a UV Mercury lamp in the block detector. When the lamp drive voltage has reached the maximum safe level (14,6V) in an attempt to make the lamp brighter, then, the lamp alarm at the front of the equipment is turned on and voltage readjustment at the lamp board is needed. When is not possible to further adjust the lamp voltage, then the lamp needs to be replaced.

Base line and baseline deviation – the base line voltage and standard deviation of output noise indicates the performance of the instruments electronics, and these values are displayed on the front instrument panel as well as in the output data. The base line should maintain a consistent small positive value. A large baseline deviation or noisy baseline could indicate problems with the lamp or other electronics.

2.2.1 Principle of operation

The 2537B features two gold cartridges. While cartridge A is adsorbing mercury during a sampling period, cartridge B is desorbed and analyzed. The roles of the cartridge are then reversed. The system is in many ways similar to a thermal desorption system for VOCs or halocarbons. This alternate action allows continuous sampling of the inlet stream. The length of exposure and the flow rate during the adsorb phase is determined by the current operational method.

Below on fig. 14, we can see an overall flow diagram of the instrument. Solenoid V1 is used to select between ambient air (in the normal OFF state) and external zero air (ON state). Zero air is introduced into the instrument during the following conditions:

- Cartridge clean operation
- Zero phase of calibration
- Span phase of calibration
- External zero control bit is activated

Solenoids V2 and V3 are switched together and select between the two cartridges. In the OFF state, cartridge A is being adsorbed (exposed to air) and cartridge B is being fed carrier gas. In the ON state, the situation is reversed.

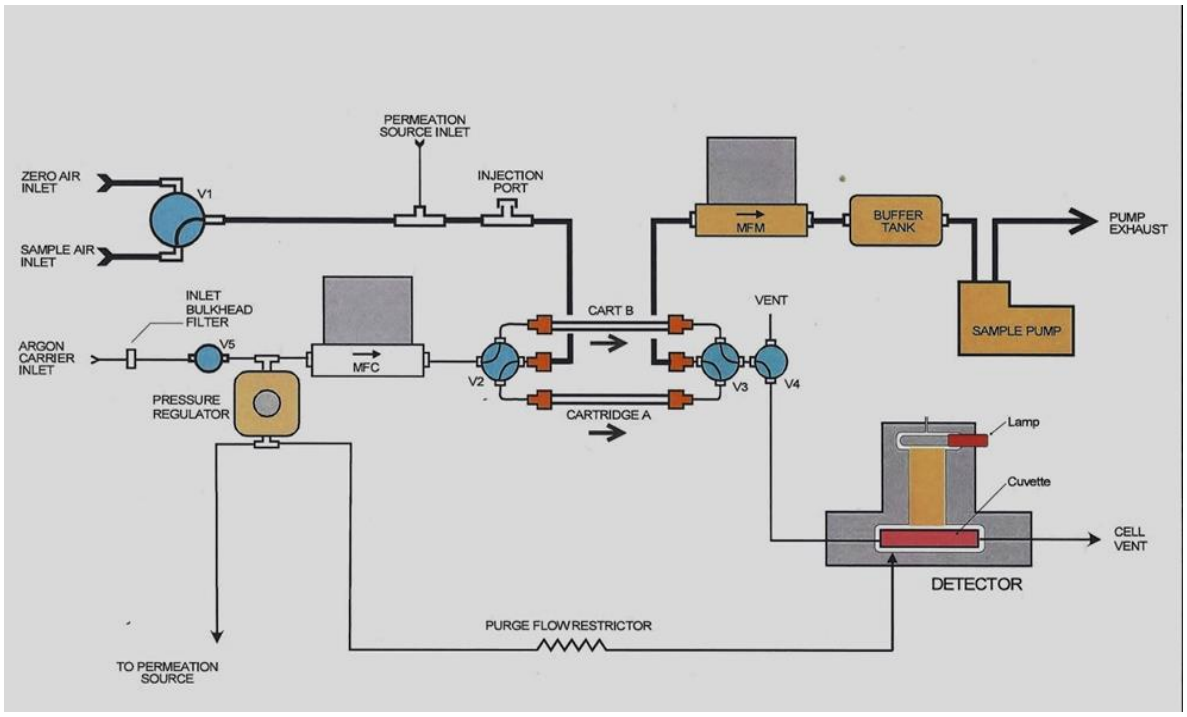

Figure 14. *Overall flow diagram (taken from TEKRAN user manual)*

After completion of a sampling period, the A/B solenoids change state. The Bypass solenoid V4, is activated at this time. The cartridge that is to be analyzed is now flushed with carrier gas, and the effluent air is vented to the atmosphere. This venting through V4 prevents the detector cell from being contaminated by the effluent. After flushing is complete, V4 is deactivated and the carrier gas passes through the detector.

Stainless steel solenoid, V5 is a cut off valve that automatically turns the carrier gas supply to the instrument on and off as power is applied. This prevents the carrier flow during a power failure or when the instrument is turned off. The carrier is then split into two streams.

One stream delivers a controlled flow to the cartridge currently being desorbed and hence the detection cell. The carrier gas mass flow controller (MFC) allows greatly reduced carrier usage and shorter cycle times. The MFC is set to the following levels during a desorption cycle:

- During the initial **Flush phase** of a desorption cycle, the controller is set to allow a very large carrier flow. This allows rapid clearing of air out of the cartridge and surrounding fittings, allowing quicker cycles.

- During **Base line** and **Peak** acquisition, the carrier flow is set so as to produce optimally shaped peaks.
- During **Cool-Down** and **Idle** periods, the flow is set to a very low value. This flow is just sufficient to keep the lines and detection cell flushed and stable.

Carrier gas is also delivered to a precision pressure regulator. The regulators provide a fixed pressure that is applied to a set of three capillary tube flow restrictors. The first of these is used to deliver carrier gas at low rate (approximately 10 ml/min) to the optical path of the detection cell. The remaining two restrictors provide specific flows to the permeation source.

2.2.1.1 Detector

Fig.15 below shows a cross section of the detector. The cell uses Cold Vapour Atomic Fluorescence Spectrophotometry (CVAFS) for the detection of mercury. In addition to being much more sensitive than atomic absorption, the phenomenon is linear over a much wider range and not as subject to positive interferences. The major negative interference mode is quenching caused by the presence of molecular species.

All desorption operations are performed in an inert, ultra high purity Argon carrier gas. The adsorption step uses pure gold as the adsorbent. This material is highly specific to mercury, reducing interferences.

Mercury that was adsorbed onto the gold matrix is released during heating in Argon. The mercury is carried into a quartz cuvette illuminated by a low pressure mercury vapor lamp. Radiation at 253.7 nm excites any mercury atoms present, which fluoresce and re-radiate at the same wavelength. A photomultiplier tube (PMT) views the cell through a monochromatic filter at right angles to the incident light. Direct light from the source is not seen by the PMT, however, the fluorescence produced by the mercury in the cuvette is observed by the PMT. The intensity is directly proportional to the amount of mercury in the cuvette.

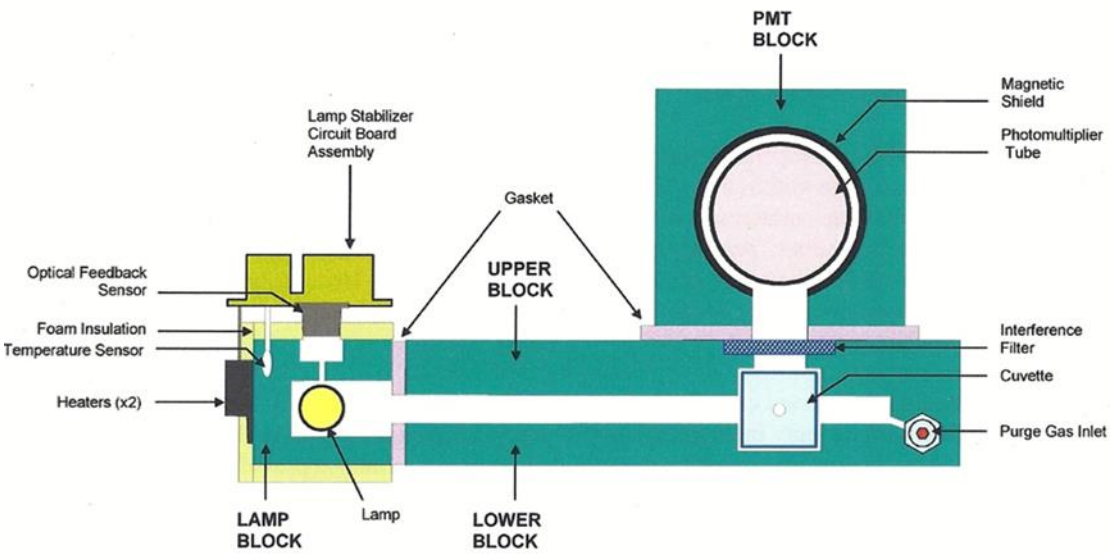

Figure 15. *Detector assembly (side view) (taken from TEKRAN user manual)*

2.2.1.2 Lamp Stabilizer

All model 2537B analyzers are equipped with a Lamp Stabilizer. The circuit board for this stabilizer is mounted directly on top of the lamp block. A temperature sensor and heaters keep the entire block at a constant temperature. A photodiode with an internal interface filter is used to monitor the output of the lamp at 253.7 nm. The drive voltage is adjusted to keep the output of the lamp constant. Indicator lights on the board show the current status of the heaters and whether the lamp has aged beyond the ability of the controller to maintain a constant intensity. Under normal operation, the red LED should be off and the yellow LED on.

2.2.1.3 Permeation Source

The instrument is equipped with a permeation source. This source provides a stable, repeatable alternative to calibration by manual injection. Fig.16 illustrates the construction of the source.

A precision temperature controlled aluminium block containing the permeation chamber is maintained to within 0.05 ^{o}C of the setpoint, resulting in stable emission rates. The range of allowable temperatures is from 45 to 75 ^{o}C, with 50 ^{o} being the normal setting. A variety of permeation tubes, ranging in length from 1 to 4 cm may be installed in the chamber to accommodate a variety of calibration concentration. Using tubes of different construction allows an even wider range of permeation rates. Glass beads and glass frit serve to preheat

the chamber purge gas. In order to prevent contamination and eliminate any possibility of oxidation on the permeation tube surface, only inert gas is used to provide a continuous purge flow. A capillary restrictor, fed by a pressure regulator provides this constant flow. When the source is inactive, the purge flow (approximately 30 ml/min) is routed to the external **Perm Vent** through solenoid V6. The source is activated by:

- A source calibration span operation
- The rear panel Source control bit

This latter capability allows the manual "spiking" (standard additions) of ambient or zero air samples.

When the source is activated, solenoid V6 is turned on. This causes the perm chamber output to be injected into the sample path. Solenoid V6 is a special three-way solenoid with an extra port. In the OFF position it routes the perm chamber output to the external **Perm Vent**, where it is trapped onto a charcoal filter. The ports of V6 are configured so as to provide a direct path through the solenoid body. When source injection is complete, V6 is turned off. Valve V7 is then activated for a short period of time to ensure that the entire source delivery pathway is thoroughly flushed. This prevents residual amounts of mercury in the transfer line from contaminating subsequent samples.

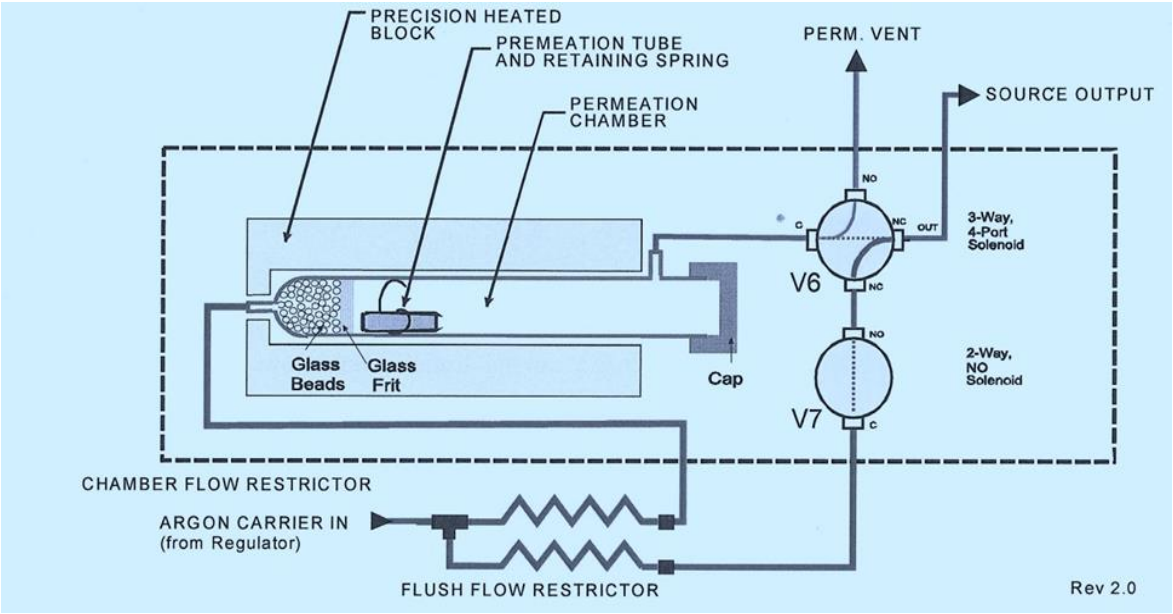

Figure 16. *Permeation source flow diagram (taken from TEKRAN user manual)*

3. Results and Discussion

We present here data from the 1st January 2012 to the 1st April 2014. Fig 17 show mercury time series raw data plot with the base line and baseline deviation. Those are important parameters during the QA/QC procedure.

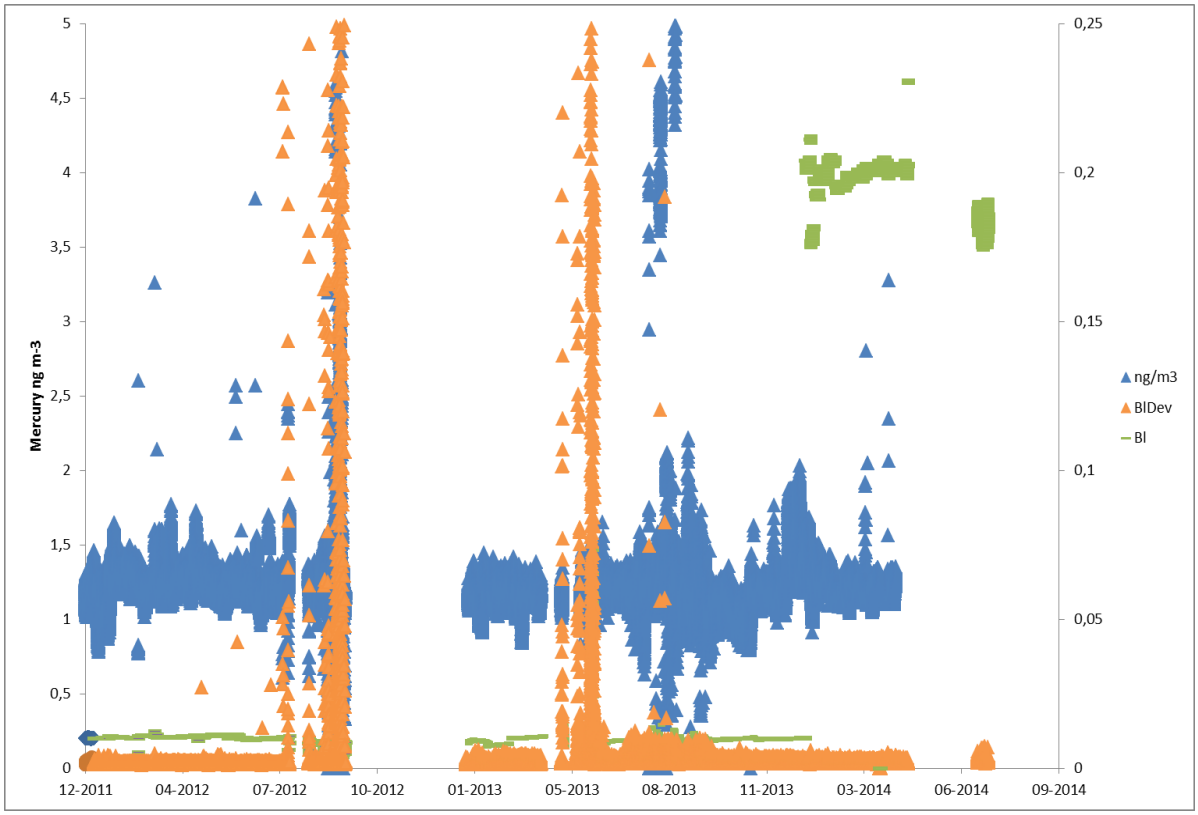

Figure 17. *TGM concentration (blue line), Base line (orange) and base line deviation (Yellow) for measurements made at the Cape Verde Observatory.*

What is visible on Fig. 17 are sudden drops in the signal baseline, that should have stable values between 0.100 – 0.250V, and a large increase in baseline deviation (which should be less than 0,100V, for a well performing system providing clean and valid data). When data fail to match those parameters, they should not be validated, and this is visible when comparing the raw data from plot on Fig 17, with the data after QA/QC procedure on plot on Fig 18.

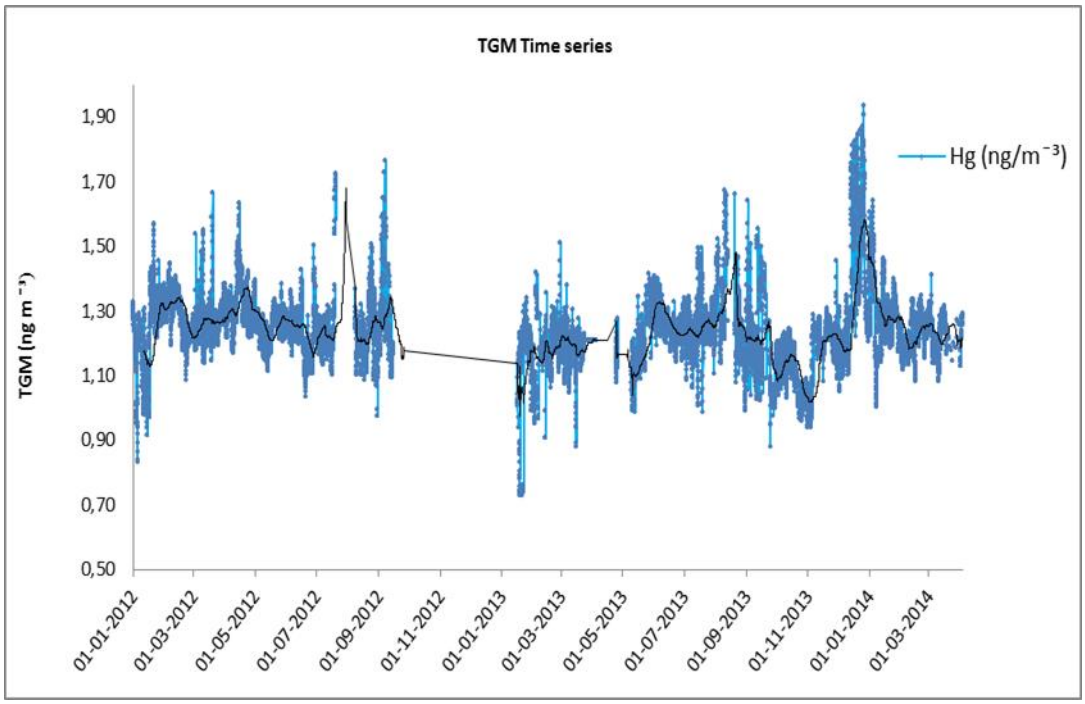

Figure 18. *Total Gaseous Mercury time series from the Cape Verde Atmospheric Observatory, over period Jan 2012 to Apr 2014. Data shown is hourly averaged (blue) with a 2 week running mean (black line).*

Observing the CVAO TGM time series plot, Fig 18, we can see that most of the time, the Mercury concentration is between 1.0 and 1.4 ng m^{-3}. Due to its relatively long residence time in the atmosphere, the ground level background concentration tends to be relatively constant over hemispheric scales. When compared with measurements from cruise campaigns from North to South Atlantic, (Table 3) we can see that the CVAO TGM data (table 4) is similar to previously reported southern Atlantic data, where Hg concentrations are lower than the northern part of the Atlantic.

Being distant from the major important anthropogenic emissions sources in Europe and North America, means that despite being in the northern hemisphere, Cape Verde is at a sufficiently low latitude that data observed in CVAO is more consistent with data observed in the southern hemisphere.

Trends through the year are not so clear as we can see in Fig 18 but it's possible to see higher concentrations from July to September observed in both years 2012 and 2013, lower concentration during November 2013 but cannot compare from the previous year due to gap on data, and high concentration during a dust event from the 14th to the 18th December 2013, when CVAO is strongly influenced by air masses coming from the west coast of

Africa. The big gap on data from the 15th September 2012 to the 16th January 2013 was due to a broken pump on the inside of the instrument.

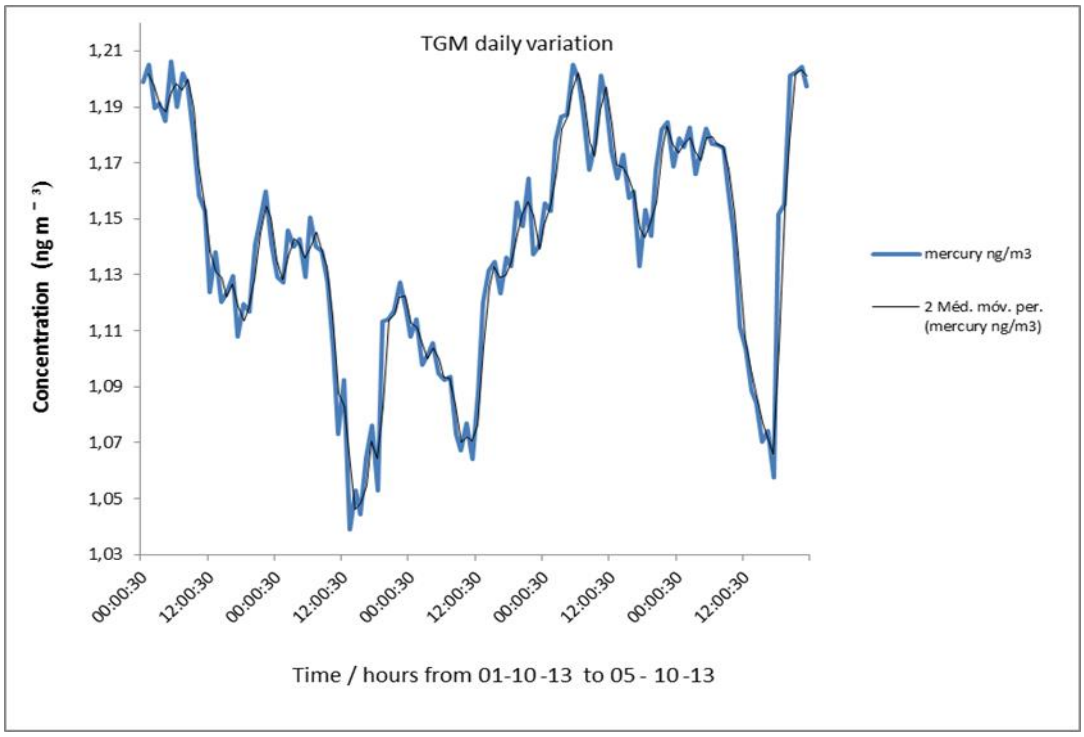

Figure 19. *Diurnal trend observed in the CVAO TGM data with increasing concentrations during the night, decreasing at the sun rise and reaching the minimum during the afternoon around 17:00h.*

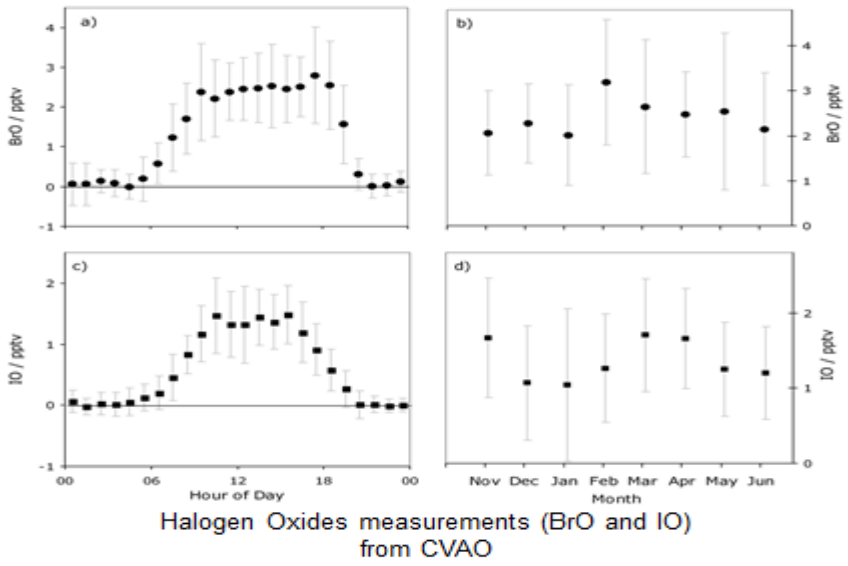

Figure 20. *Halogen Oxides (BrO and IO) from DOAS measurements in CVAO, taken from Read et ao. 2008.*

When observing diurnal cycles, strong diurnal variations can be seen in Fig. 19, (data observed for 5 days from the 1st to the 5th Oct 2013) with decreasing TGM concentration from sun-rise to the end of each afternoon, after which TGM concentrations start increasing again. The destruction of Hg during the day is consistent with loss mechanisms with both Br and OH, which have their maximum during the day. Results from previous halogen oxides measurements in CVAO represented in Fig 20, showed concentrations increasing early in the morning with a maximum around mid-day and decreasing in the evening and reaching zero during the night. TGM diurnal trends showed opposite behavior, with TGM concentrations increasing in the evening when BrO reach its minimum, start decreasing at sun rise when BrO start increasing and reaching its minimum between around 12:00h and 16:00h when BrO has its maximum concentration. Br has the potential to be the most important oxidant for the removal of GEM (that is around 95% of TGM) from the atmosphere and the mechanisms for this is showed by reaction R3 for Bromine (Br_2) and reaction R4 for Bromine Oxide (BrO), both on Table 1 earlier. OH as well is a very important oxidizing agent at the marine boundary layer and has the potential also for the removing of GEM, and the way this happen is showed on reaction R2 on table 1.

Measurements were stopped from 16th October 2012 to 17th Jan 2013 due to a problem with the internal pump, which had to be replaced. The remoteness of the observatory means that relatively straightforward component filatures can take a long time resolve, since all parts require shipping from overseas.

Moisture in the internal tubing of the analyzer during summer time when relative humidity has reached values higher than 90%, (August and September 2012 and 2013), has caused many problems with the measurements, (including the broken pump in 2012). This is a universal problem with instrumentation housed at the Cape Verde Observatory labs.

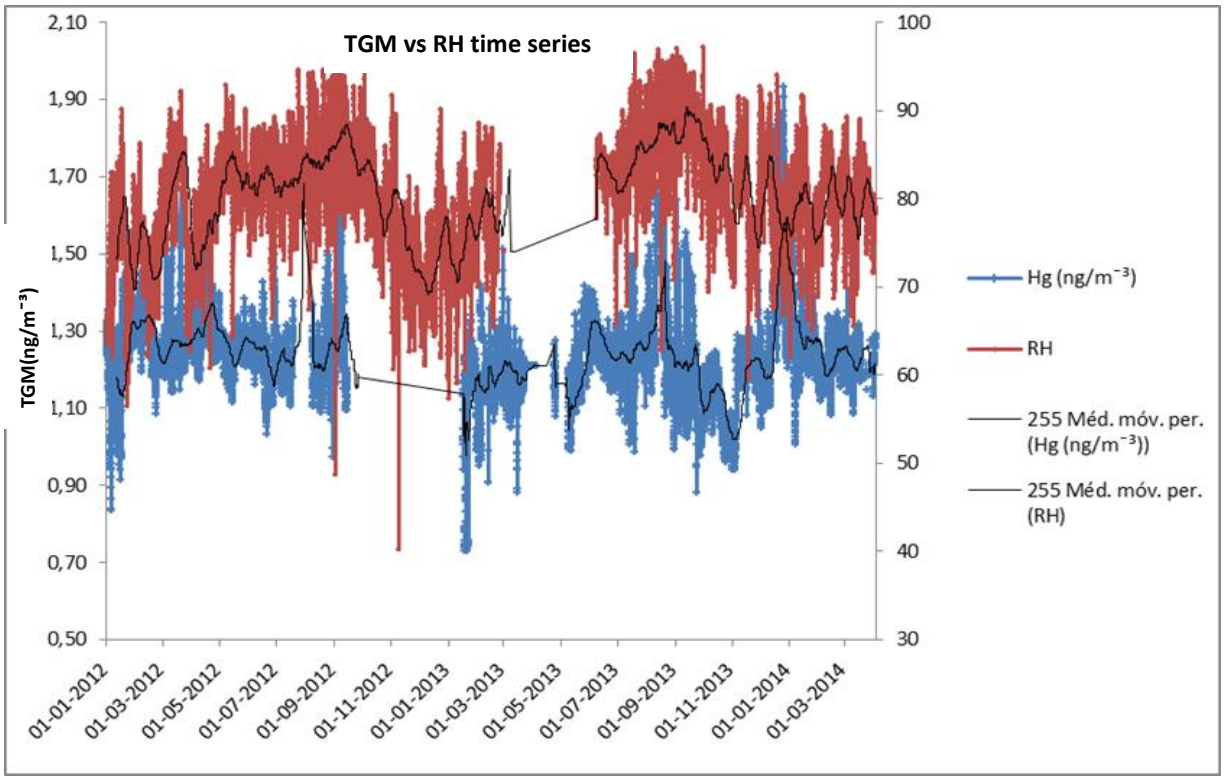

Figure 21. *TGM and RH time series 2012-2014.*

When observing TGM and Relative Humidity time series (Fig 21), it is possible to observe a positive correlation between them, and this is more evident when observed on a daily variations plot.

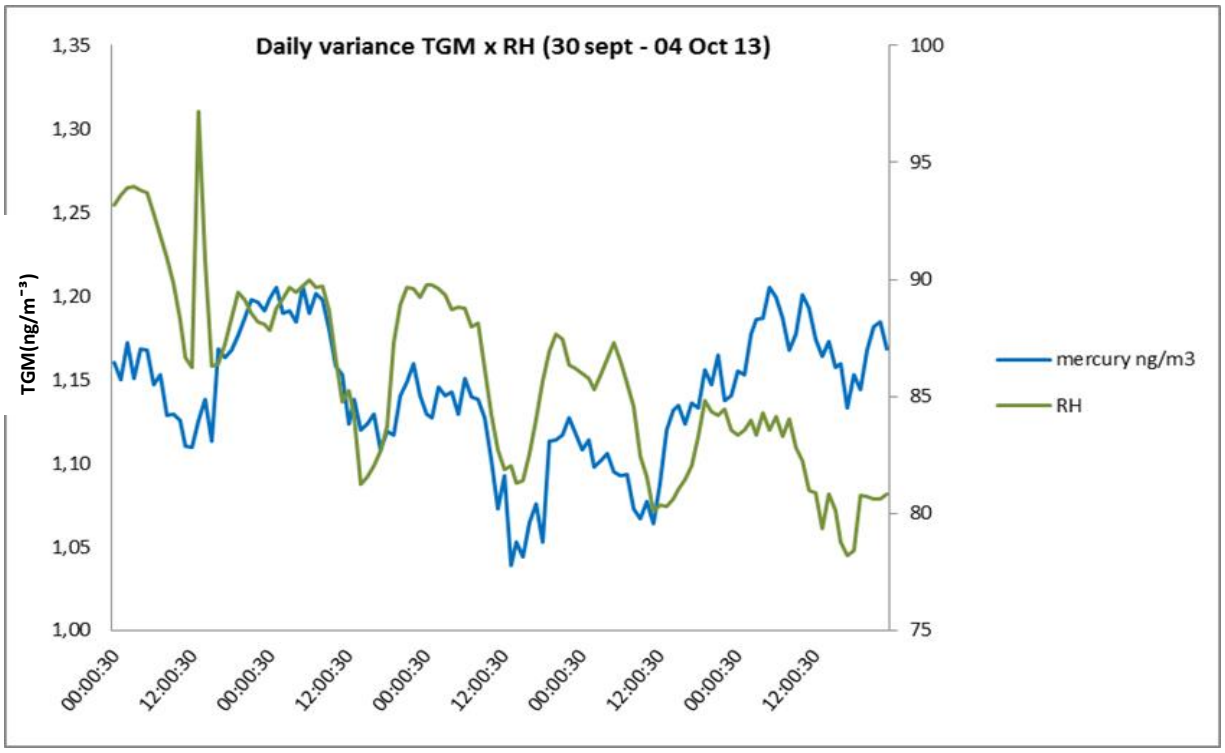

Figure 22. *TGM and RH daily variance show a positive correlation*

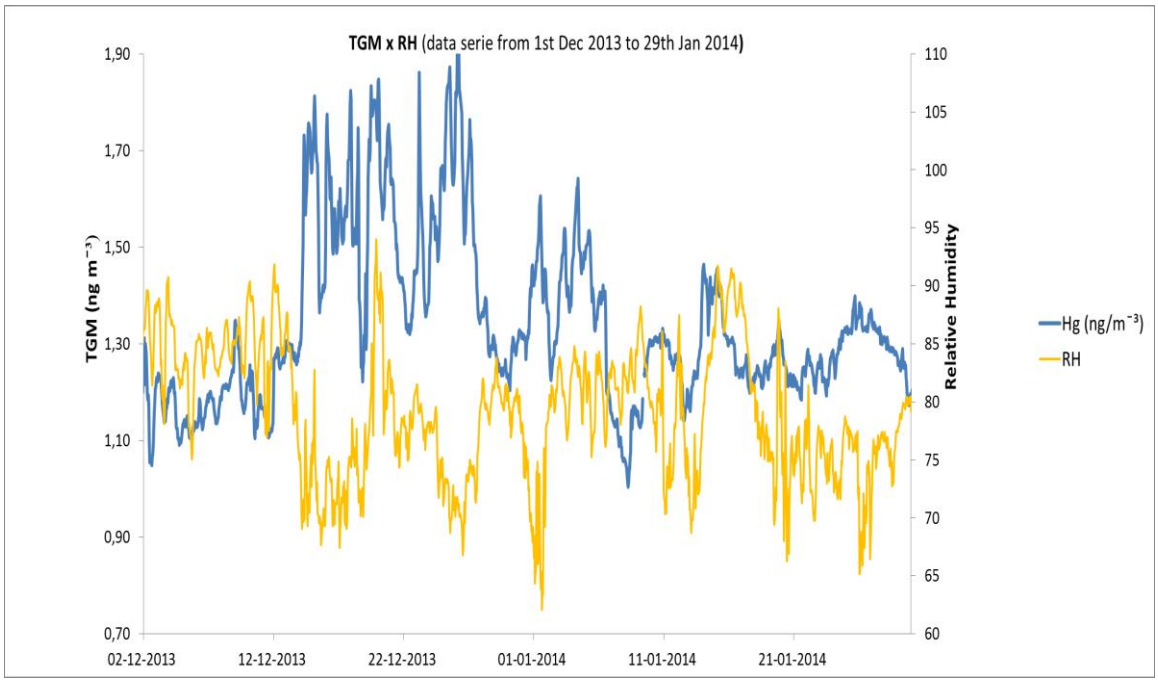

Figure 23. *TGM concentration increasing and RH decreasing during a dust storm from 13th to 27th Dec 2013 (Data series from the 1st Dec 2013to 29th Jan 2014).*

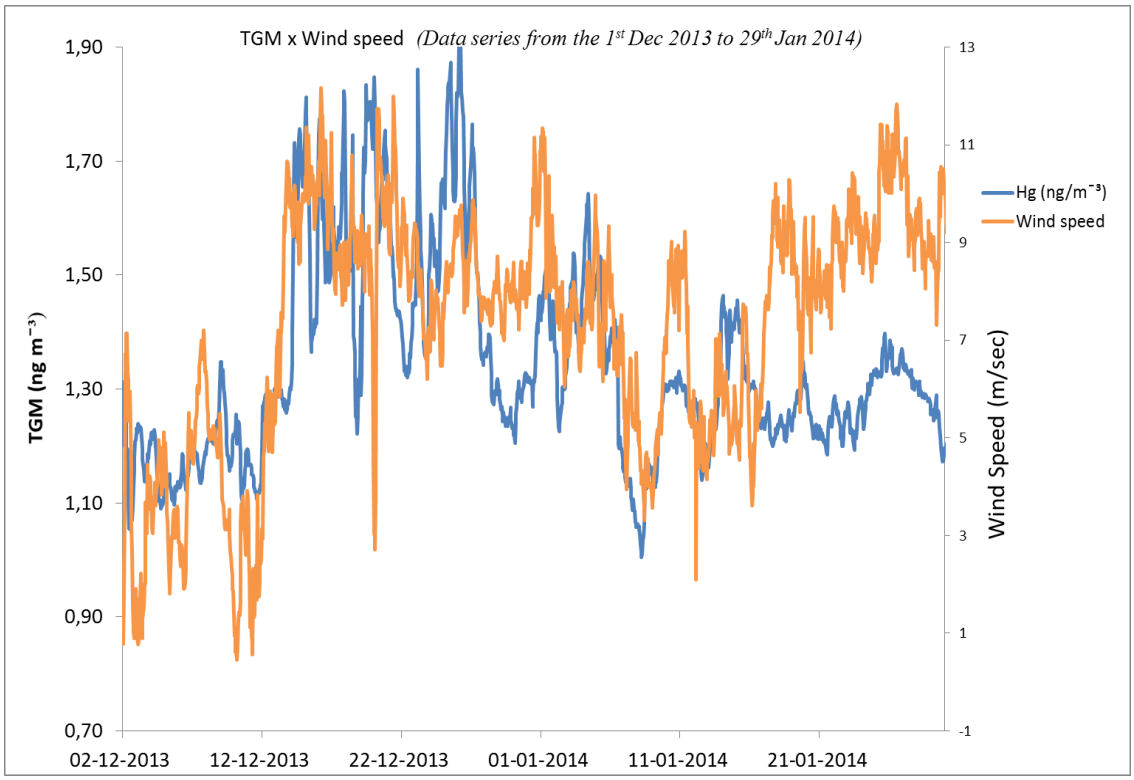

Figure 24. *TGM vs wind speed during a dust storm from 13th to 27th Dec 2013 (Data series from the 1st Dec 2013to 29th Jan 2014).*

According with measurements from 30th Sep to 04 Oct (Fig 22), Periods of higher humidity correspond with higher concentration of TGM.

But observations made during a dust storm from the 13rd to the 27th Dec 2013 have showed the opposite (Fig 23) with highest values of TGM registered when values of RH has dropped. During this same period, wind speed has increased (Fig 24), coinciding with the increase of TGM and decreasing of RH (Fig 23).

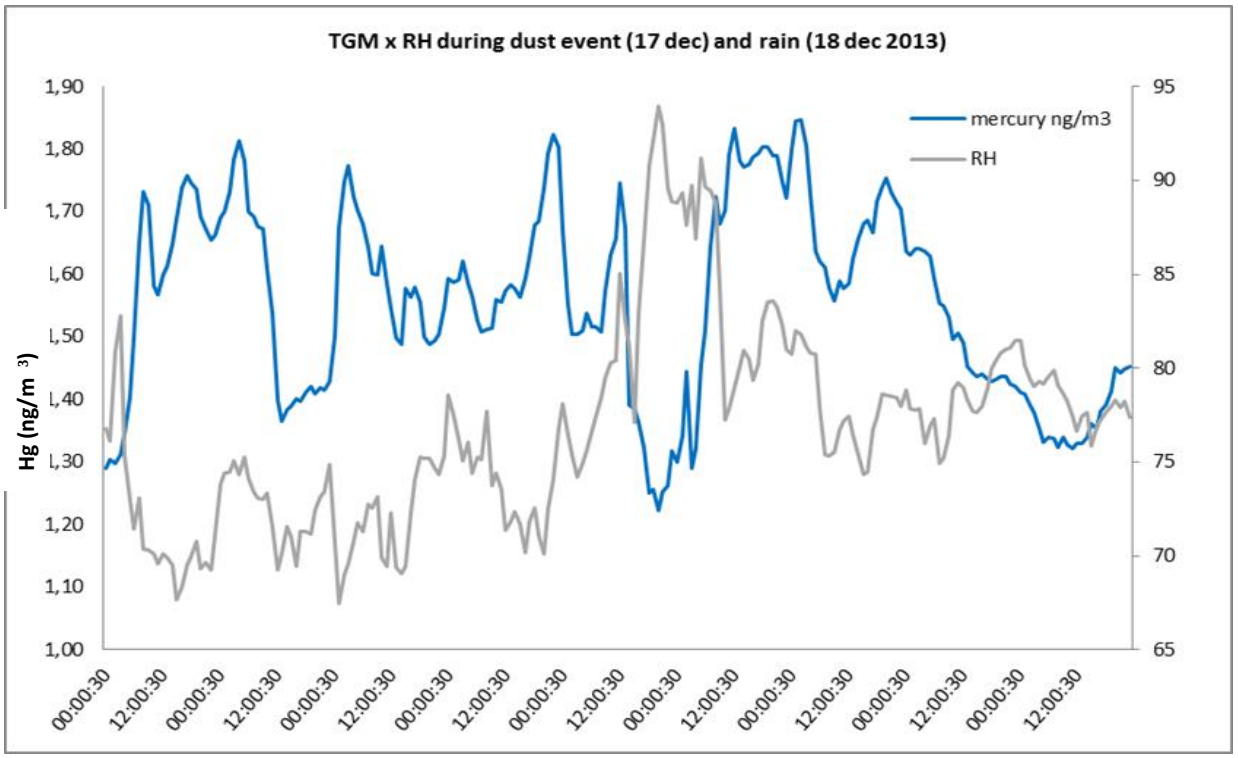

Fig 25. *Daily variance of TGM and relative Humidity during the dust event (17th Dec) followed by a quick rain event (18th Dec). Data series from the 14th to 22th Dec 2013*

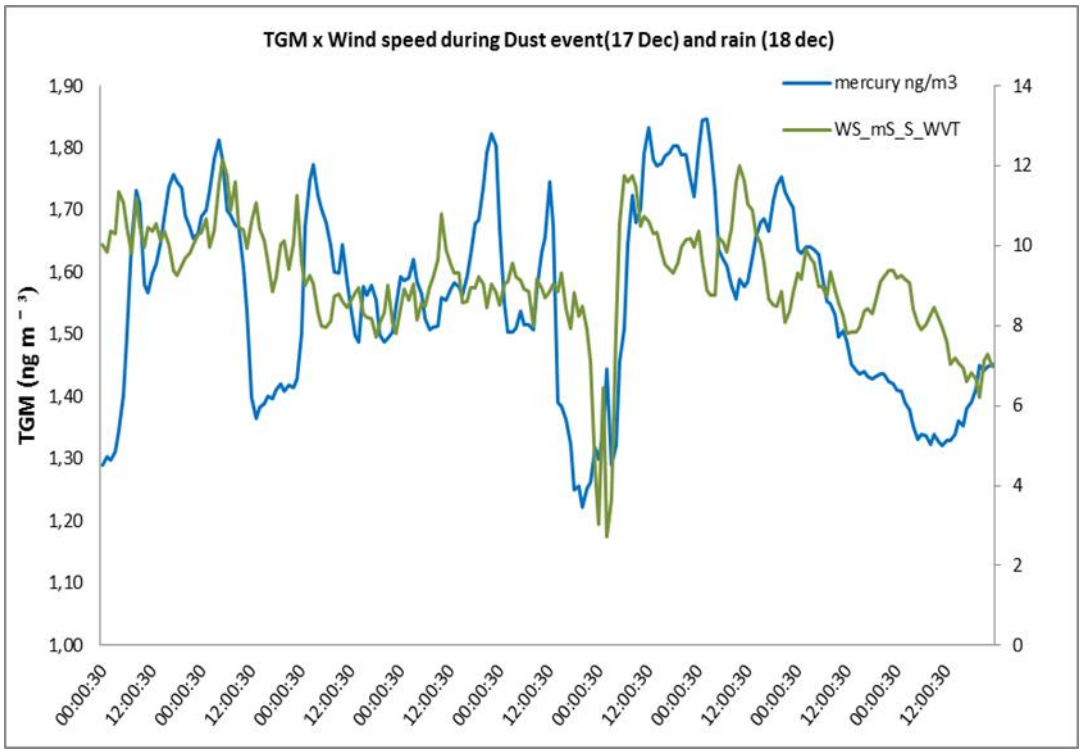

Fig 26. *TGM concentration vs wind speed during dust season from 14th to 22th Dec13*

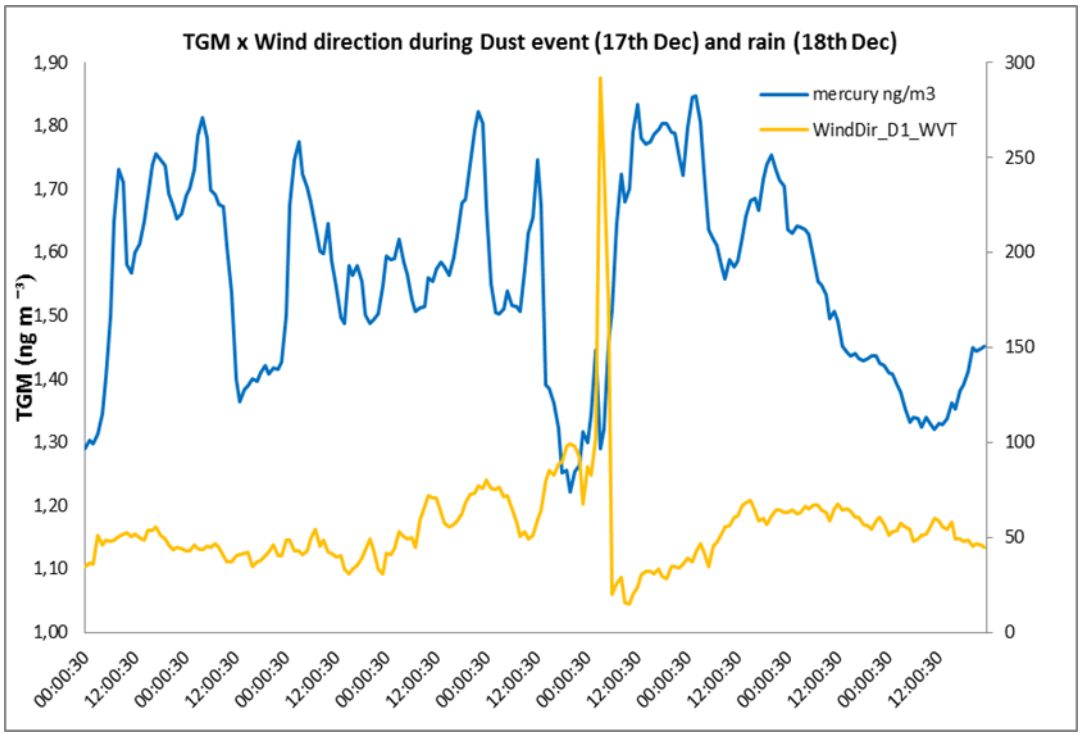

Fig 27. *TGM concentration vs wind direction during dust season from 14th to 22th Dec13*

The highest values of TGM were observed during periods of high wind speed (Fig 24, Fig 26) suggestive that TGM was coming from long-range transport from regions of anthropogenic emissions. During this period, a sudden drop of TGM concentration occurred immediately after a sudden drop on wind speed and sudden change of wind direction (Fig 27). These type of case studies show how sensitive local mercury conditions are to the prevailing meteorology.

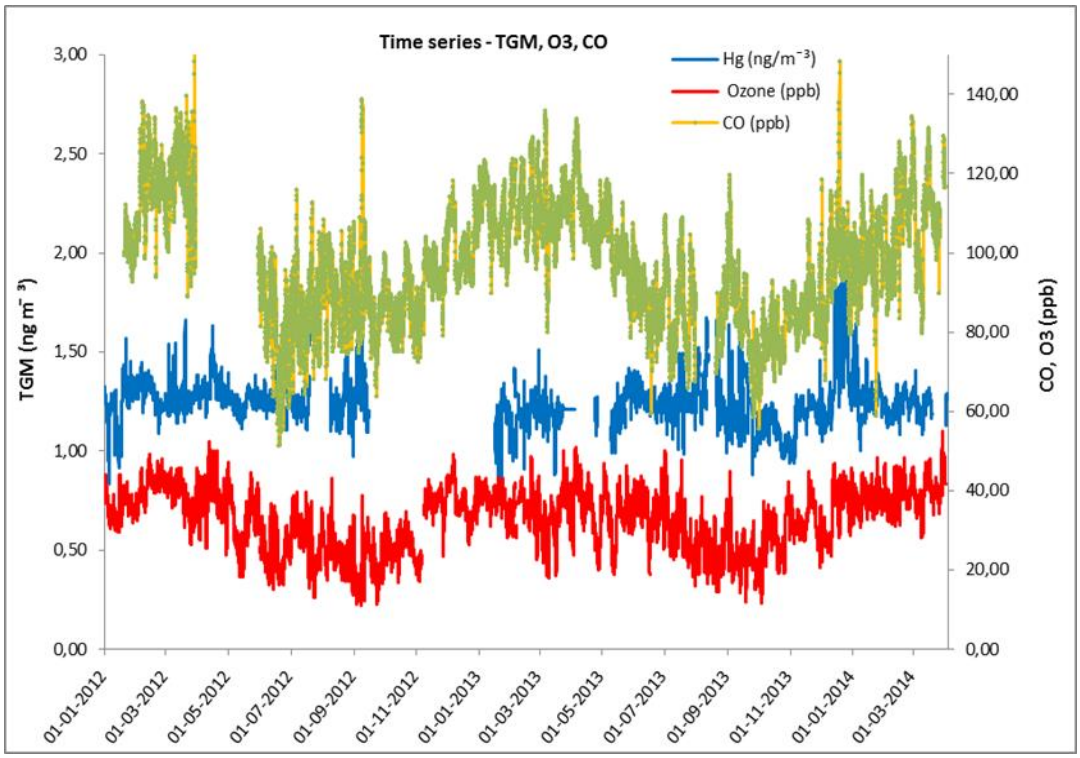

Fig 28. *Time series for TGM, Ozone and CO, period Jan 2012 – April 2014*

When comparing TGM with Ozone and CO, at the time series plot (Fig28), is not possible to observe any annual-scale correlation; There is little variability of TGM through the year, whilst CO shows an annual cycle peaking in the late winter and early spring, However whilst there is no annual correlation in their cycles, we can observe smaller or larger synoptic scale correlated events depending on the time of the year. Plots from Fig. 29 and Fig. 30 show TGM measurements from 30th Mar to 4th Apr., periods that correspond to observation of highest values of ozone and CO.

As we can see on Fig.29, CO shows a good agreement with TGM, with a positive correlation between them (Fig 31). This may attributed largely to a correlation in sources and transport – that is CO and mercury are both coming from distant anthropogenic sources and their variabilities are both controlled by transport. During this period, TGM showed a weaker diurnal profile while O_3 showed a larger depletion during the day, which may indicate the presence of halogen chemistry. Largest TGM depletions were observed on measurements from 30th Sep to 4th Oct (Fig 32, Fig 33), periods when we observe the lowest concentration values on both ozone and CO.

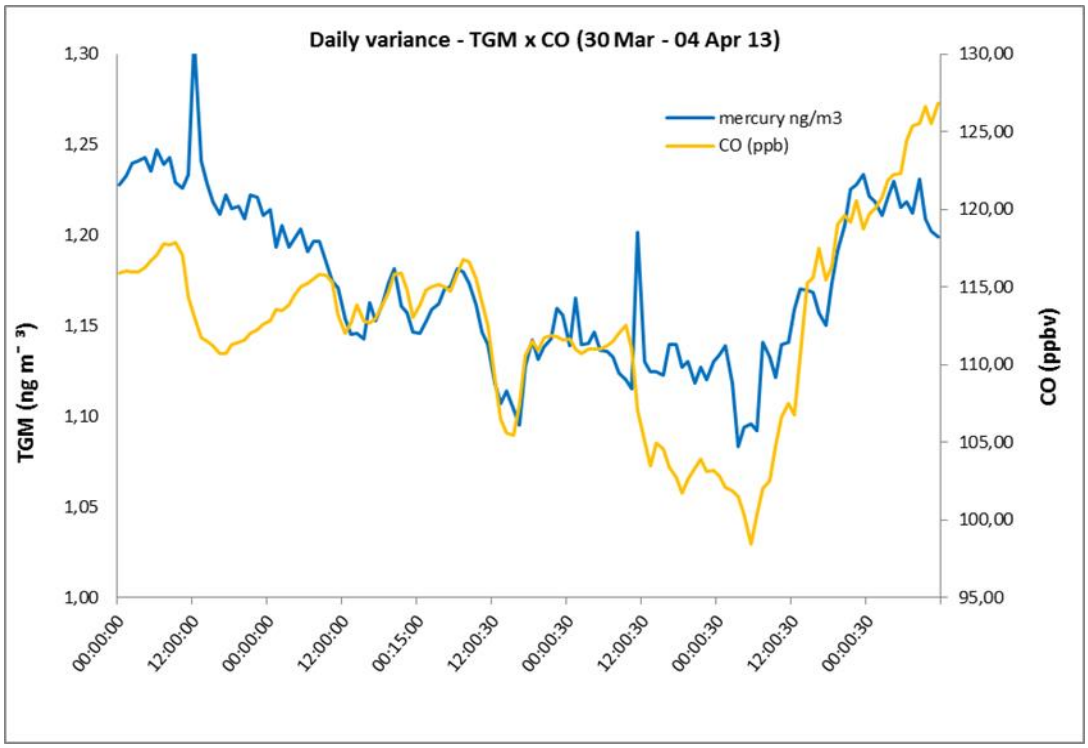

Figure 29. *Daily variance of TGM and CO, period 30 Mar – 04 April 2013*

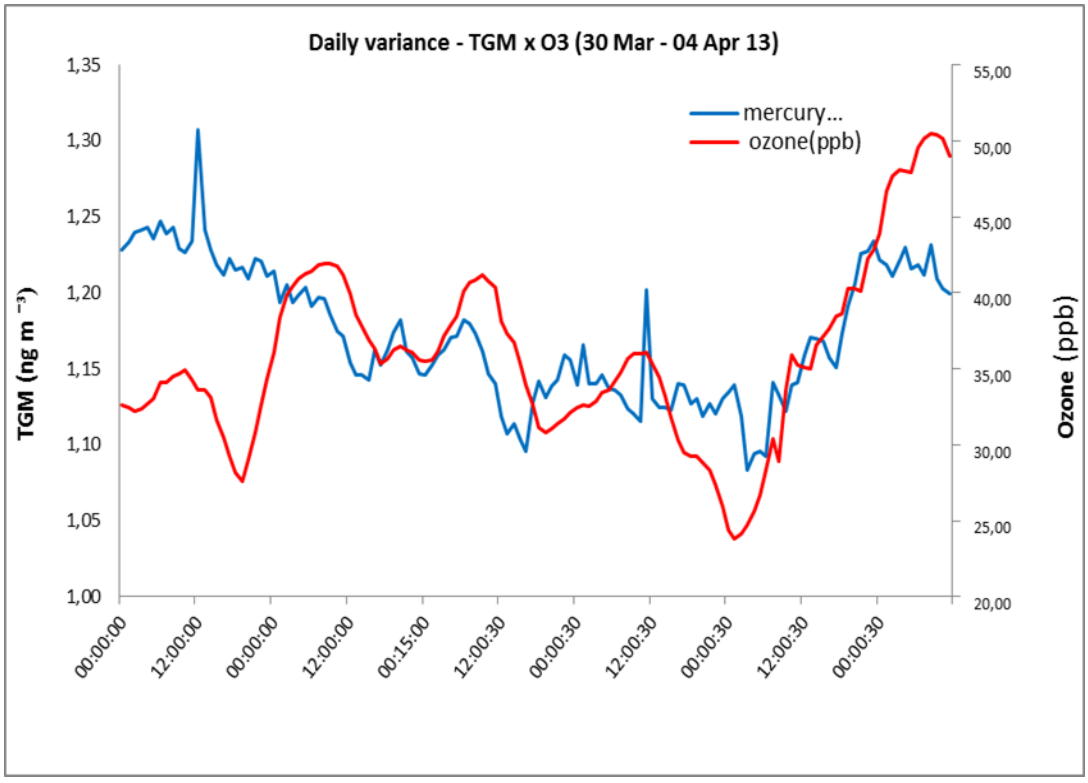

Figure 30. *Daily variance of TGM and Ozone, period 30 Mar – 04 April 2013*

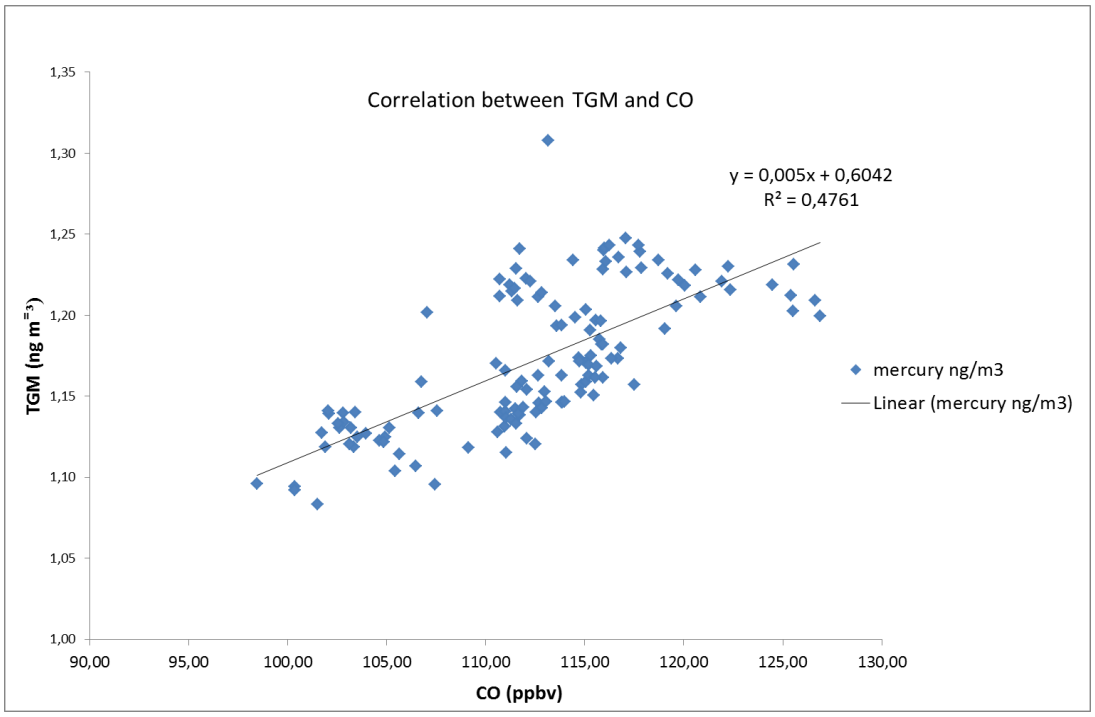

Fig 31. *Plot showing positive correlation between TGM and CO, period 30 Mar – 04 April 2013*

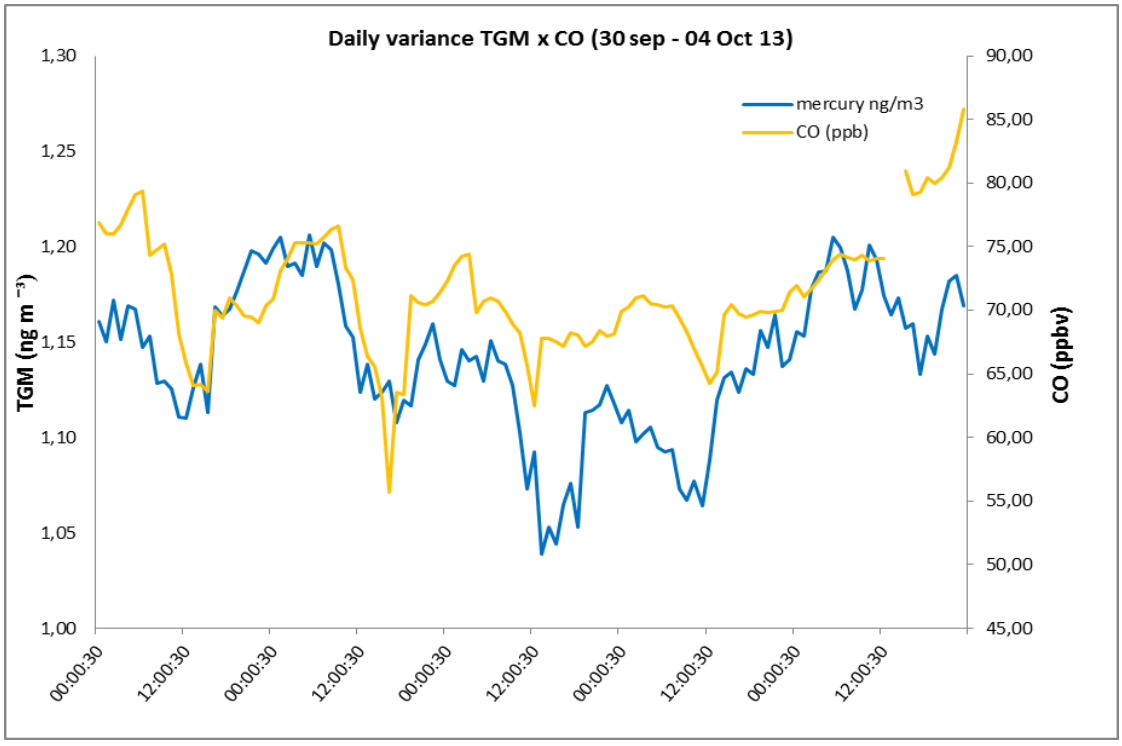

Figure 32. *Daily variance of TGM and CO, period 30 Sep – 04 Oct 13, showing a positive correlation*

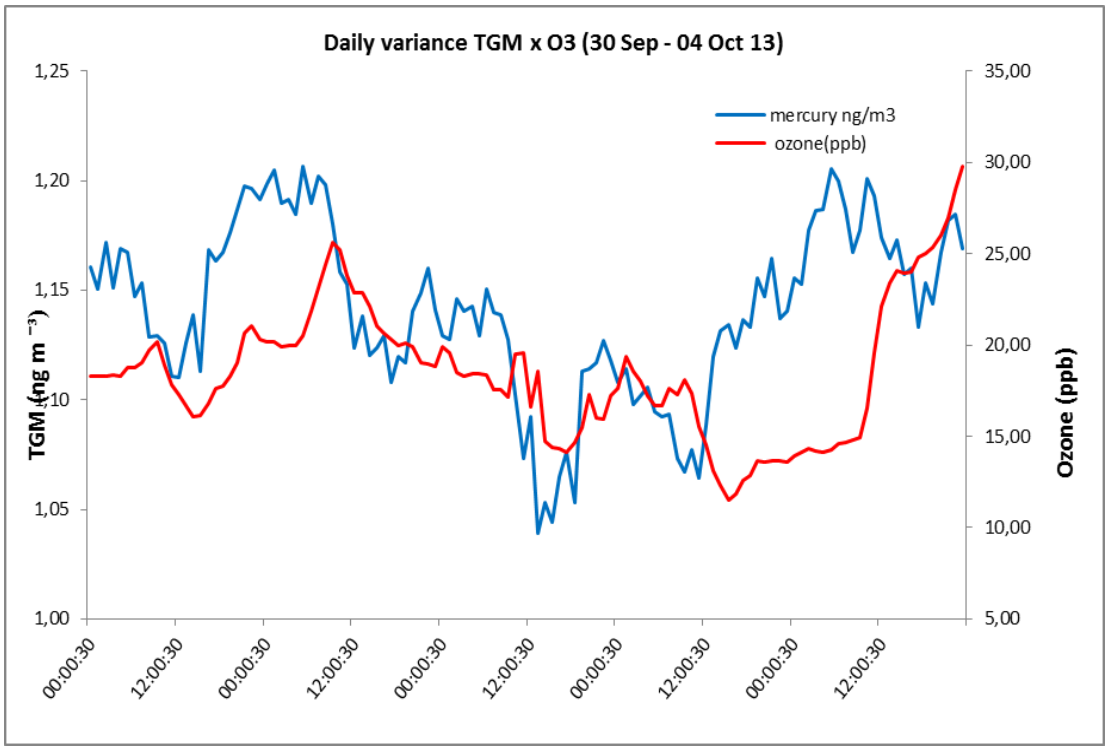

Figure 33. *Daily variance of TGM and Ozone, period 30 sept – 04 Oct 13*

A comparison of Cape Verde Atmospheric Observatory mercury values through the seasons and published literature data is shown in Tables 3 and 4. Whilst the typical values compare well between ship measurement and those made at Cape Verde, the ship data gives little information on seasonal behavior or diurnal cycles.

Table 3. *TGM measurements from Cruise campaign along the Atlantic. Table taken from Spovinieri et al., 2010*

Cruise	Range (ng m^{-3})	TGM Mean (ng m^{-3})	SD (ng m^{-3})
Atlantic Northern Hemisphere a.b			
Oct 1977	1.0 - 3.6	1.8	0.4
Nov/Dec 1978	1.4 - 2.7	1.9	0.3
Jan/Feb 1979	1.6 - 3.1	2.2	0.4
Oct/Nov 1980	1.4 - 3.4	2.1	0.4
Oct/Nov 1990	1.4 - 3.4	2.3	0.4
Oct/Nov 1994	1.3 - 3.2	1.8	0.4
Oct/Nov 1996	0.4 - 16.0	2.1	1.0
Dec 1999/Jan 2000	1.4 - 3.7	2.0	0.3
Atlantic Southern Hemisphere a.b			
Oct 1977	0.8 - 1.7	1.2	0.3
Nov/Dec 1978	0.9 - 1.9	1.4	0.2
Jan/Feb 1979	1.1 - 2.1	1.3	0.2
Oct/Nov 1980	1.1 - 1.9	1.5	0.2
Oct/Nov 1990	0.9 - 2.4	1.5	0.3
Oct/Nov 1994	0.8 - 2.1	1.2	0.2
Oct/Nov 1996	1.0 - 2.3	1.4	0.1
Dec 1999/Jan 2000	0.5 - 1.8	1.3	0.1
Feb/Mar 2000	0.2 - 1.3	1.0	0.1
Jan/Feb 2001	0.8 - 1.4	1.1	0.1

Table 4. *TGM measurements from Cape Verde Atmospheric Observatory*.

CVAO	Range ($ng\ m^{-3}$)	TGM Mean ($ng\ m^{-3}$)	SD ($ng\ m^{-3}$)
Cape Verde Atmospheric Observatory			
Jan/Fev 2012	0.83 - 1.57	1.23	0.12
Fev/Mar 2012	1.09 - 1.45	1.29	0.07
Mar/Apr 2012	1.14 - 1.66	1.27	0.07
Apr/May 2012	1.17 - 1.63	1.32	0.07
May/Jun 2012	1.11 - 1.40	1.25	0.05
Jun/July 2012	1.03 - 1.50	1.23	0.07
July/Aug 2012	1.10 - 1.72	1.24	0.10
Aug/Sep 2012	0.80 - 1.51	1.23	0.09
Sep/Out 2012	1.09 - 2.19	1.30	0.14
Jan/Fev 2013	0.65 - 1.34	1.14	0.15
Fev/Mar2013	0.91 - 1.51	1.18	0.09
Mar/Apr 2013	0.88 - 1.38	1.19	0.05
Apr/May 2013	1.08 - 1.28	1.19	0.03
May/Jun 2013	0.99 - 2.13	1.24	0.21
Jun/July 2013	1.14 - 1.41	1.26	0.05
July/Aug 2013	0.82 - 1.49	1.25	0.08
Aug/Sep 2013	0.99 - 1.90	1.29	0.14
Sep/Oct 2013	0.88 - 1.83	1.19	0.13
Oct/Nov 2013	0.94 - 1.24	1.11	0.07
Nov/Dec 2013	0.94 - 1.46	1.18	0.09
Dec13/Jan 14	1.05 - 1.93	1.38	0.21
Jan/Fev 2014	1.00 - 1.64	1.29	0.10
Fev/Mar 2014	1.08 - 1.35	1.22	0.05
Mar/ Apr 2014	1.08 - 1.41	1.23	0.05
Apr/May 2014	1.13 - 1.29	1.23	0.05

4. Conclusions

The Cape Verde Atmospheric Observatory, as a land based station in the middle of the tropical North Atlantic, facing the open ocean wind, can provide a unique insight into atmospheric mercury in the region. The region has been very under-sampled in the past. The lack of local anthropogenic sources means that observations are representative of the natural atmosphere, plus the atmospheric transformation of pollution from distant sources.

An observatory infrastructure has been used to make online continuous measurements of mercury using an analytical technique that combines gold adsorbent traps with Cold Vapour Atomic Fluorescence Spectrophotometry (CVAFS). The method has been validated, and then quality controlled over a period of two years. Whilst the instrument suffered a number of internal component failures a high coverage of data was still obtained. The data capture rate was similar to other insturments at the observatory, which is a location that is very harsh on instruments due to high levels of UV, salt, temperature and humidity, as well as physical remoteness and limited power supply.

The data, when combined with measurements from ship cruises crossing from North to South, gives a better measure of the behaviour of Mercury in tropical oceans areas, and helps resolve some uncertainties associated with emission and deposition processes. Measurements made in 2012 and 2013 are broadly consistent with cruise track measurements in terms of absolute concentration values. The equatorial location of Cape Verde means that whilst it is notionally in the Northern hemisphere, atmospheric concentrations observed in this study are closer to those seen in the cleaner southern hemisphere.

Mercury shows little atmospheric variability through the year, but does have a strong diurnal cycle reaching a minimum in the later afternoon. On many occasions the behavior of mercury is closely correlated with other long lived pollution tracers such as CO. Events such as Saharan dust transport and wind windspeed airmass transport from Europe all create unusual behaviour in atmospheric mercury.

The destruction of Hg is seen on many occasions during the day at Cape Verde, although the rate of loss is not constant. A loss of atmospheric mercury during the day is consistent with loss mechanisms with bromine and OH, which also have maxima during the day. The station is now provided with a precipitation collector that soon will improve capacity for

Mercury measurements, to include also mercury lost from atmosphere by deposition processes. Work is ongoing to install a new instrument which gives speciation of various other types of mercury, expanding the data beyond just TGM.

5. Glossary

AMAP – Artic Monitoring and Assessment Program

AMDEs – Atmospheric Mercury Depletions Events

ASGM – Artisanal and Small Scale Gold Mining

Br – Bromine atom

BrO – Bromine oxide

CH_4 – Methane

ClO – Chlorine oxide

CO – Carbon monoxide

CO_2 – Carbon dioxide

CVAFS – Cold Vapor Atomic Fluorescence Spectrometry

CVAO – Cape Verde Atmospheric Observatory

DOAS – Differential Optical Absorbance Spectroscopy

FAO – Food and Agriculture Organization

GAW – Global Atmospheric Watch

GEM – Gaseous Elemental Mercury

GEOS – Global Earth Observation System of Systems

GMOS – Global Mercury Observation System

Hg – Mercury

Hg^{II} – Divalent mercury compounds

HgOH – Mercury hydroxide

$HgCl_2$ – Mercury chloride

HO_2 – Hydroperoxyl radical

INMG – Instituto Nacional de Meteorologia e Geofísica

IO – Iodine oxide

LED – Light Emitting Diode

MBL – Marine Boundary Layer

MFC – Mass Flow Controller

NO – Nitrogen oxide

NO_2 – Nitrogen dioxide

N_2O – Nitrous oxide

O_3 – Ozone

OH – Hydroxyl radical

PMT – Photo Multiplier Tube

PTWI – Provisional Tolerable Weekly Intake

QA/QC – Quality assurance/Quality control

RGM – Reactive Gaseous Mercury

RH – Relative Humidity

SF_6 – Sulfur hexafluoride

TGM – Total Gaseous Mercury

TPM – Total Particulate Mercury

UNEP – United Nations Environmental Program

UV – Ultraviolet

WHO – World Health Organization

WMO – World Meteorological Organization

VOCs – Volatile Organic Compounds

6. List of References

AMAP/UNEP, *Techical Background Report to the Global Atmospheric Mercury Assessment. Artic Monitoring and Acssessment Programe/UNEP Chemicals Branch*; 4, 65-69, 84. 2008.

Aspmo et al., Environ. Sci. and Technol, 40, 13, 4083-4089, 2006.

Ariya et al., Book Series: Advances in Quantum Chemistry Volume: 55 Pages: 43-55 , 2008

Barrie et al., Nature, 334, 138-141, 1988.

Brooks et al., Geophys. Res. Lett., 33, 13:L13812, 2006.

Calvert and Lindberg, Atmos. Environ., 38, 5105-5116, 2004.

Calvert and Lindberg, Atmos. Environ., 39, 18, 3355-3367, 2005.

Christensen et al., Atmos, Chem. Phys., 4, 2251-2257, doi:10.5194/acp-4-2251-2004, 2004.

Cobbet et al., Atmos. Environ. 41, 31, 6527-6543, 2007.

Dastoor and Larocque, Atmospheric Environment, 38, 147-161, 2004.

Dibble et al., Atmos.Chem. Phys., 12, 10271-10279, doi:10.5194/acp-12-10271-2012, 2012

Douglas et al., Geophysical research Letters, 32, 4, 2005.

Ebinghaus et al., Environ. Sci. Technol., 36, 1238-1244, 2002

Ferrara et al., Sci, Total Environ., 213:13-23, 1998.

Fitzgerald et al., Science, 224, 597-599, 1984.

Gardfeldt and Jonsson, J. Phys. Chem. A, 107, 22:4478-4482, 2003.

Goodsite et al., Environ. Sci. Technol., 38, 1772-1776, 2004.

Goodsite et al., Environ. Sci. Technol., 46, 5262-5262, 2012

Hedgecock et al. J. Geophys. Res.: Atmospheres, 111, D20, 27, 2006.

Hedgecock and Pirrone, Environ. Sci., Technol., 38, 69-76, 2004.

Holmes et al., Geophys. Res., 33, L20808, doi:10.1029/2006GL027176, 2006.

Holmes et al., Atmos. Chem. Phys., 10, 12037-12057, doi:10.5194/acp-10-12037-2010, 2010.

Kim and Fitzgerald, Science, 231, 1131-1133, 1986.

Kim and Kim, J. Environ. Sci. Helath.-Part A, 31, 8, 2023-2032, 1996.

Laurier and Mason, J. Geophys Res., 112, D06302, doi:10.1029/2006JD007320,2007.

Laurier et al., J. Geophys. Res., 108, 4529, doi:10.1029/2003JD003625, 2003.

Lin et al., Atmos. Environ., 40,16, :2911-2928, 2006.

Lindberg et al., Environ. Sci. Technol., 36, 1245-1256, 2002.

Lindberg et al. Ambio, 36, 19-32, 2007.

Muller at al., Atmos.Chem.Phys., 12, 7391-7397, doi:10.5194/acp-12-7391-2012, 2012

Munthe, Nature, 355, 434-437, 1992.

Obrist et al., Nature Geoscience, 4, 22-26, 2011.

Pal and Ariya, Environ. Sci. Technol., 38, 5555-5566, 2004

Pirrone N and Mason R. *Mercury Fate and Transport in the global Atmosphere: Measurements, Models and Policy Implications 2008*; xxxv; 1-2

Pirrone et al. Springer, chap, 23, 541-579, 2005.

Pirrone et al., chap. 1, pp. 1-47, Springer, http://dx.doi.org/10.1007/978-0-387-93958-2_7,ISBN:978-0387-93957-5, 2009

Platt et al., Atmos.Chem.Phys., 4, 2393-2399, doi:10.5194/acp-4-2393-2004, 2004.

Read et al., Nature, vol 453; 1234. 2008.

Saiz-Lopez et al., Atmos. Chem.Phys., 8, 887-900, doi:10.5194/acp-8-887-2008, 2008.

Saiz-Lopez and von Glasow, Chem. Soc. Rev. 41, 6448-6472, doi:10.1039/c2cs35208g, 2012.

Schoroeder et al., Atmos. Environ., 29, 809-822, 1998.

Simpson et al., Atmos. Chem. Phys., 7, 4375-4418, doi:10.5194/acp-7-4375-2007, 2007.

Sorensen et al., Environ. Sci. Technol., 44, 7425-7430, 2010a.

Soerensen et al., Environ. Sci. Technol., 44, 8574-8580, 2010b.

Sorensen et al., Environ.Sci.Technol., 47, 7757-7765, 2013.

Sprovieri F et al., Atmospheric Chemistry and Physics; 8245-2050, 2010.

Sprovieri F et al., Atmospheric Chemistry and Physics, 3985, 2010.

Steffen et al., Atmos. Chem. Phys., 8, 1445-1482, doi:10.5194/acp-8-1445-2008, 2008.

Stephens et al., J, geophys. Res: Atmos., 117, D14, 27, 2012

Strode et al., Global Biogeochem. Cy., 21, GB1017, doi:10.1029/2006GB002766, 2007.

Sunderland and Mason, Global Biogeochem. Cycles, 21(4):GB4022., 2007.

TEKRAN, 2003. Ambient Mercury Vapor Analyzer. User Manual; Chapters 1-1, 1-4, 1-5, 1-6, 1-7, 1-8.

The Global Mercury Observation System. Available at: http://www.gmos.eu

Theys et al., Atmos Chem. Phys., 11, 1791-1811, doi:10.5194/acp-11-1791-2011, 2011.

Tuckermann et al., Tellus 49b, 533-555, 1997.

F. Wang, A. et al., Atmospheric Chemistry and Physics; 1323-1335, doi:10.5194/acp-14-1323-2014, 2014.

Wanberg et al., Atmos. Environ., 41, 2612-2619, doi:10.1016/j.atmosenv.2006.11.024.2007, 2007.

Weiss-Penzias et al., Environ. Sci. Technol., 37, 17, 3755-3763,2003.

Yang et al. J. Geophys. Res., 110 (D23):D23311, 2005.